Life-history evolution and local adaptation under seasonal disruptions

by

Rebekah Anna Hall

B.Sc., University of Alberta, 2022

Thesis Submitted in Partial Fulfillment of the
Requirements for the Degree of
Master of Science

in the
Department of Mathematics
Faculty of Science

SIMON FRASER UNIVERSITY

Summer 2024

Declaration of Committee

Name:	**Rebekah Anna Hall**
Degree:	**Master of Science**
Thesis title:	**Life-history evolution and local adaptation under seasonal disruptions**
Committee:	**Chair:** Jessica Stockdale Assistant Professor, Mathematics
	Ailene MacPherson Supervisor Assistant Professor, Mathematics
	Ben Ashby Committee Member Associate Professor, Mathematics
	JF Williams Committee Member Associate Professor, Mathematics
	Leithen M'Gonigle Examiner Associate Professor, Biological Sciences

Abstract

Life-history traits, such as those determining an organism's fecundity (the parameter r) and ability to compete for resources (the parameter K) demonstrate unique eco-evolutionary feedback loops due to their direct relationship to individual fitness. Classic theory holds that in a constant environment, evolution will maximise an individual's competitive ability. However, many environments undergo seasonal changes which may alter these evolutionary pressures. Spatial heterogeneity in seasonal disruptions may result in local adaptation and spatial polymorphisms of these life-history traits. In this thesis, I consider life-history evolution in a Lotka-Volterra model with three different types of seasonal perturbations: fluctuating death rates, fluctuating resource levels, and repeated, sudden crashes in population size. Using asymptotic approximations and Floquet analysis on the long-term periodic solutions, I show that fluctuating resources cannot change the evolutionary outcome, but that sufficiently harsh population crashes or fluctuating death rates will favour increased fecundity over competitive ability. Finally, I apply both a deterministic impulsive differential equation model and stochastic simulations to study local adaptation of an island population to periodic population crashes in an island-mainland model. I find that local adaptation favouring r-selected individuals once again arises when conditions are sufficiently harsh, but not so harsh that the island population cannot be sustained in the absence of migration.

Keywords: life history; local adaptation; eco-evolutionary dynamics; seasonality; r/K selection; population genetics models

Dedication

To my mom, whose passion for science is the reason I am where I am today.

Acknowledgements

First and foremost I would like to start by thanking my supervisor, Ailene MacPherson, for all of her support over the last two years. An additional thanks must go to Ben Ashby for his feedback on this thesis. I would also like to express my gratitude to all my lab mates for their feedback on my presentations and writing, as well as for their support.

A big thanks to all the undergraduate professors who encouraged me to continue on with my studies. Thank you especially to Daniel Charlebois for giving me my first research opportunities and to Jay Newby for introducing me to the field of mathematical biology. J'aimerais aussi remercier Filsan Ahmed Youssouf, dont le cours de calcul est la raison pour laquelle j'ai fait mon baccalauréat en mathématiques. Or in English, I would also like to thank Filsan Ahmed Youssouf, whose calculus course is the reason I started my bachelor's degree in mathematics.

I also have so much gratitude for all my friends and family. Thank you to everyone in my office for making such an amazing community here at SFU. Thank you to Elisha and Kirsten for always being there to pick me up whenever I visited home, both figuratively and literally from the airport. Thank you to Maddy for her constant support and for pushing me to become a better writer. Thank you to Josiah for always grounding me in what's most important. Thank you to my grandparents, who have done so much to support my education. And finally, thank you to my parents. You have worked so hard to help me become a person who could leave and do interesting things, for which I am eternally grateful. I hope you know that no matter how far I go, I'll always come back.

Table of Contents

List of Tables

List of Figures

Chapter 1

Introduction

The fields of ecology and evolution are inextricably linked: ecological pressures mediate selection on phenotypes according to their relative fit to an environment. How ecology shapes evolution is critical to informing theoretical and predictive frameworks for understanding evolutionary processes. Life-history theory aims to understand this link between ecology and evolution by examining how traits which determine demography—that is, those relating to reproduction, growth, and mortality—evolve under specific environmental conditions and how this gives rise to the observed diversity of life history traits across environments and species [58].

Classic theory holds that in a constant environment, long-term evolution will maximise competitive ability even at the cost of reproductive ability [39]. However, this may not be the case in the presence of noisy or seasonal environments. Seasonal disruptions can come in a variety of forms. A population may undergo sudden, recurring population crashes, such as a population of pathogens exposed to regular doses of an antimicrobial drug [69]. Alternatively, disruptions may change continuously over time, with good seasons and harsh seasons due to changing mortality or resource levels [6, 14]. In many cases, populations exist in multiple environments with different seasonal patterns [12]. This may result in local adaptation, in which a population adapts to its local environmental conditions, often at the expense of its success in other environments [5].

Roughgarden (1971) considered seasonal population crashes in the context of overwintering, where there are a limited number of available spaces for hibernation, forcing the population down to a fixed size after each winter. Using a discrete-time model, they showed

that such seasonal forcings could be sufficient for high-reproductive strategies to persist in a population. The goal of this thesis is to expand this theory to a continuous-time framework and consider additional forms of seasonal disruptions. Additionally, I seek to understand how local adaptation of life-history traits is shaped by seasonal disruptions by introducing spatial structure.

In Chapter 2, I give a review of the literature on life-history theory and selection in temporally-variable and spatially-structured environments. In Chapter 3, I consider evolution of life-history traits in a single population subject to three different seasonal perturbations: regular population crashes, periodically-changing death rates, and periodically-changing resource levels. In Chapter 4, I use both deterministic analysis and stochastic simulations to study local adaptation of life-history traits to an island experiencing seasonal population crashes. I conclude in Chapter 5 with an overview of my results and a discussion of limitations and future work.

Chapter 2

Literature Review

2.1 Life-history theory

2.1.1 A framework for modelling life-history evolution

The framework of r- vs. K- selection has been a foundational concept in the development of life-history theory. MacArthur and Wilson (1967) first introduced this framework by describing the colonisation of an island [40]. Initially, resources on the island are abundant and there is no need for competition, thus organisms with a high rate of reproduction (r-selected) will begin to take over. However, with time the population will grow, depleting local resources and increasing competition for these resources. This results in a shift in the selection exerted on the population as those with a greater competitive ability (K-selected) will prevail [52]. The theory of r- vs. K- selection is thus one of density-dependent selection, where changes in the population density mediates the direction and strength of natural selection and therefore evolution [43]. The two life-history strategies show contrasting patterns of density dependence, with the fitness advantage of high rates of reproduction decreasing with increasing density (negative density-dependence) while the fitness advantage of high competitive ability increases with density (positive density-dependence), as shown in Figure 2.1 [53].

Anderson (1971), Charlesworth (1971), and Roughgarden (1971) presented some of the earliest mathematical models of density-dependent selection, which quantified MacArthur and Wilson's scenario described above: assuming a constant environment, individuals with a high competitive ability—that is, a large K—would prevail [2, 8, 53]. This can be seen in Figure 2.2. For a more in-depth analysis of these patterns of density dependence, see

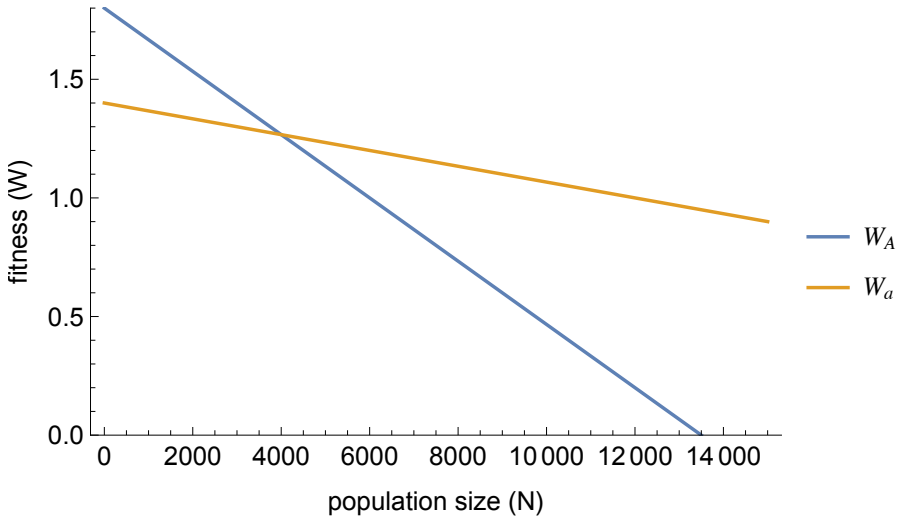

Figure 2.1: **Density-dependent selection on r versus K traits.** The fitnesses of a high-r/low-K A allele and a high-K/low-r a allele as a function of population density (N). While the absolute fitness of both traits decreases with increasing N, the high-r allele becomes steadily less advantageous and eventually deleterious as determined by its fitness relative to that of the high-K allele. Parameter values are as follows: $r_A = 0.8$, $r_a = 0.4$, $K_A = 6000$, and $K_a = 12\ 000$.

Appendix A.1. These early observations highlighted how the selective advantages of certain traits may depend on the environment: ecology influences evolution [52].

2.1.2 Choosing a model: discrete vs. continuous time

An important consideration when modelling density-dependent selection is the choice between modelling in discrete versus continuous time. Continuous-time life-history models are appropriate for systems where reproduction among individuals is asynchronously occurring throughout time. Continuous-time models are formulated using differential equations. Discrete-time models, which are formulated using difference equations, capture systems with synchronous reproduction and mortality events. Analogous continuous and discrete models which use the same values for growth, carrying capacity, or other relevant parameters will display similar behaviours, such as having the same equilibria, but can otherwise differ in their behaviour, reflecting fundamental differences in the underlying biological processes [41]. They also differ in the available mathematical analyses and hence their mathematical tractability. Although analogous models will have the same equilibria, the stability of these equilibria will not necessarily be the same. Discrete models have been shown to be

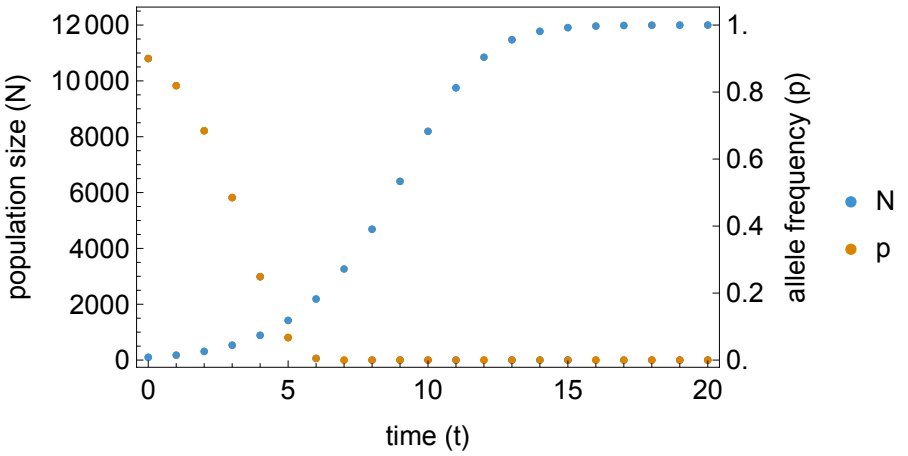

Figure 2.2: **Dynamics of population size and allele frequency in a discrete-time haploid model.** Parameter values are as follows: $r_A = 0.8$, $r_a = 0.6$, $K_A = 11\ 000$, and $K_a = 12\ 000$, $N(0) = 100$, $p(0) = 0.9$. Allele frequency is of the high-r allele A.

generally less stable than continuous models; while stability in a discrete model will imply stability in the analogous continuous model, the reverse is not necessarily true [41].

Discrete and continuous models also use different definitions of fitness. Discrete models use the Wrightian definition of fitness (W_i):

$$N_i^{t+1} = W_i N_i^t.$$

Here W_i can be interpreted as the number of individuals with genotype i there will be in the next generation for every one individual having genotype i in the previous generation [49]. These difference equations may be rewritten in terms of the change in the total population size (N) and in the frequency of a given allele (p). Then the selection coefficient (S) for that allele is defined by the equation:

$$p^{t+1} - p^t = Sp^t(1 - p^t).$$

For a biallelic, haploid population, the discrete selection coefficient for the A allele would be given by:

$$S_A = \frac{W_A - W_a}{\bar{W}},$$

where:

$$\bar{W} = W_A p^t + W_a(1 - p^t).$$

The continuous analogue of Wrightian fitness is Malthusian fitness (m_i):

$$\frac{dN_i}{dt} = m_i N_i.$$

Malthusian fitness is interpreted as the continuous growth rate of the genotype i population [49]. Once again, the differential equation model can be rewritten as differential equations for the total population density (N) and allele frequency (p), and the selection coefficient (S) is defined by:

$$\frac{dp}{dt} = Sp(1 - p).$$

The continuous selection coefficient for the A allele in a biallelic, haploid population is given by:

$$S_A = m_A - m_a.$$

Both W_i or m_i may be functions of N (density-dependent), of p (frequency-dependent), or both. The patterns of density- or frequency-dependence between analogous discrete and continuous fitnesses (and their corresponding selection coefficients) will often be the same (see Appendix A.2.2 for example). The relationship between the Wrightian fitness (W) in a discrete model and the Malthusian fitness (m) of the analogous continuous model is given by the logarithmic transformation [10, 49]:

$$m = \ln W.$$

This nonlinear relationship can result in differences in the behaviour of the discrete model as opposed to the continuous. However, these differences become less as selection becomes weaker. In this case, the relationship between m and W becomes approximately linear, and the behaviour of the analogous discrete and continuous models will more closely resemble each other [10, 49].

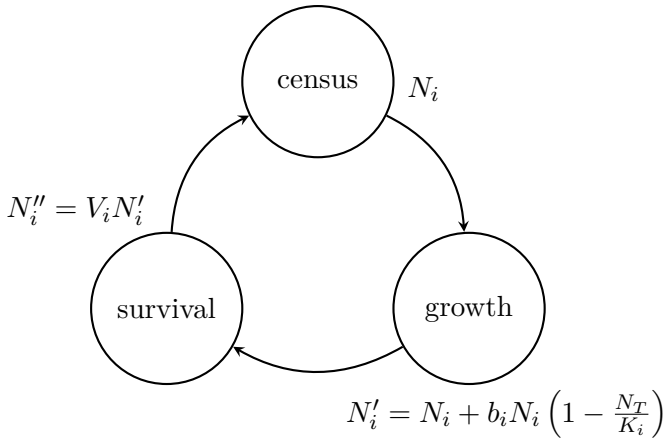

Figure 2.3: **Single life-cycle for a haploid population with survival.** N_i is the number of individuals with allele i, N_T is the total population size, and K, b, and V represent carrying capacity, birth rate, and viability respectively.

2.1.3 Density-dependent fitness and density-dependent selection

The terms "r-selection" and "K-selection" are derived from the classic formulation of the logistic model of population growth in which r is the intrinsic growth rate of the population and K is its carrying capacity. While this is the most frequently used model of density-dependent selection, it does not capture the full range of density-(in)dependence acting on traits. To facilitate a full contrast between positive and negative density-dependent and density-independent selection let us consider an extension of the classic logistic model (shown in Figure 2.3) with three life-history traits: birth rate (b), viability (V), and carrying capacity (K). Using the life-cycle shown in Figure 2.3, we consider a population that first experiences a growth/reproduction step in which individuals reproduce in a density-dependent manner as a function of their genotype i according to the classic logistic growth model (with the growth rate r replaced with a birth rate b). Following this growth phase, individuals must survive the remainder of the season/year and do so with a genotype-dependent probability V_i. Incorporating these two steps into a single equation, we have that the number of individuals carrying allele i after a single time step is given by:

$$N_i^{t+1} = V_i \left[1 + b_i \left(1 - \frac{N_T^t}{K_i}\right)\right] N_i^t. \tag{2.1}$$

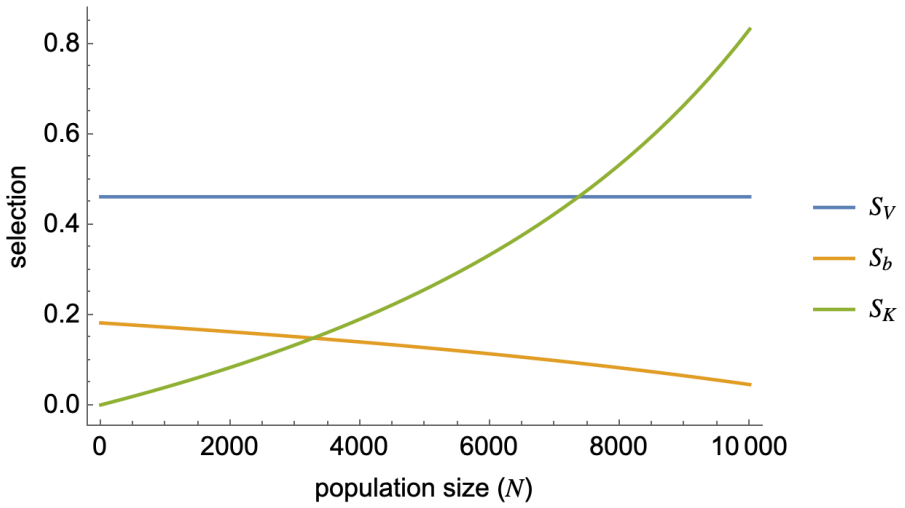

Figure 2.4: **Selection coefficients for individual life history traits of $b/V/K$ growth model for a haploid population.** Parameter values are as follows: when only viability differs, $V_A = 0.5$ and $V_a = 0.8$; when only birth rate differs, $b_A = 0.5$, $b_a = 0.8$, and $K = 12\,000$; when only carrying capacity differs, $K_A = 6000$, $K_a = 12\,000$, and $b = 0.8$. In all cases, allele frequency was $p = 0.5$.

where N_T^t is the total population size which includes individuals with all possible alleles. A more detailed description of the model can be found in Appendix A.2.1.

This extension reveals an instance where a trait which confers fitness in a density-dependent manner does not experience density-dependent selection (shown in Figure 2.4). Birth rate and carrying capacity display both density-dependent fitness and selection as in the logistic model, but this is not the case for viability. While fitness is still density-dependent, when only the viability is allowed to differ between alleles, the selection coefficient is independent of the population size (see Appendix A.2.1 for proof).

2.1.4 Life-history trade-offs

Much of life-history theory relies on the presence of trade-offs between different life-history traits [43]. Without trade-offs, long-term evolution would inevitably aim to maximise all traits which contribute positively to fitness and minimise all traits which contribute negatively [34]. This is a trivial conclusion, and fails to explain the diversity of life-history strategies observed throughout nature. By introducing trade-offs, the question of which traits will be maximised by long-term evolution becomes an optimisation problem [58].

As discussed above and in Appendix A.1, despite the prevalence and importance of life-history trade-offs in other areas of life-history theory, it has been shown that in a simple

model of a haploid population experiencing logistic growth in a constant environment, long-term evolution will always select for the allele with the highest carrying capacity, regardless of the nature of the trade-off between r and K. This is also the most common outcome for a diploid population, with the exception of a handful of cases when the heterozygote's phenotype exceeds that of both homozygotes (overdominance) [53]. Given that trade-offs alone are insufficient to explain the coexistence and variation of r vs. K strategies, additional processes must be included. One possible process is temporal environmental variation, a case we explore in detail below [34, 53].

Modelling life-history trade-offs is not limited to a trade-off between r and K. In fact these values can be best understood as emergent properties of traits such as fecundity, survival, or body size. Such traits will vary throughout an organism's lifetime and may be subject to trade-offs between each other: trade-offs which themselves may vary between age stages [35, 52, 58]. These traits all contribute and respond to population density differently. They may also respond differently to spatial or temporal variation in the environment, as may the nature of the trade-offs between them [35, 57]. Thus in studying life history evolution, one must consider a wide range of trade-offs between different life-history traits, as well as interactions between these trade-offs with age and environment.

2.1.5 Quantitative traits

The models cited thus far have considered the evolution of a single gene which determines traits such as a growth rate and carrying capacity and thus the fitness of the individual. One method for studying population growth and evolution according to a collection of particular traits which contribute to fitness is by modelling the evolution of phenotypes as opposed to genotypes. Quantitative genetic models describe the parameters of a growth model as functions of a list of quantitative traits—such as egg size and egg number in birds—and analyse the selection pressures on these traits and the evolution of the population as a whole [32]. As they are based on phenotypes, these models must consider both the genetic and environmental contributions to the traits. Consideration of trade-offs is also inherently built into the model, as it must define the matrices of genetic and environmental correlations between traits, which act as trade-offs [32].

2.2 Density-dependent selection in temporally-variable environments

2.2.1 Motivation

An important driver of genetic diversity is environmental variability, as populations must respond to the ever-changing evolutionary pressures that arise around them [9, 26, 66]. The conclusion of traditional population genetic models has been that genetic polymorphisms can arise from negative frequency-dependent selection but not from temporal environmental variation alone [71]. However, these models ignore ecological factors such as competition for resources. When taking these into consideration, it can be shown that stable polymorphisms can arise in a population [71]. This raises the question of how life-history traits, which are fundamentally tied to these ecological mechanisms, will evolve under a temporally-changing environment. Indeed, the evolution of density-dependent traits has been well-known in ecology to be dependent on changes in the population size caused by changes in the environment [15, 53].

Environmental variation may occur on a number of time scales and with varying degrees of predictability, from rapid, random changes in a noisy environment to slow, periodic changes in a seasonal environment. The relationship between changing environments and life-history evolution is also of greater interest as climate change leads to increased environmental variability, with seasonal changes becoming more dramatic and unpredictable and environmental conditions becoming noisier [13, 56].

2.2.2 Evolution in periodic environments

Periodic environment models describe systems where environmental conditions change according to deterministic cycles. These periodic environments can drive periodic population dynamics, which often lead to density-dependent feedback loops. Thus, an organism's life history is closely tied to how it will respond to periodic variations in the environment [9]. Similarly, periodic environments can induce species coexistence or stable polymorphisms between organisms with different life histories which are each more advantageous during different seasons [66].

Recent experimental work with *Drosophila melanogaster* showed rapid adaptation of individuals to seasonal changes and supported the important role of seasonality in maintaining genetic diversity [54]. Observations of *D. melanogaster* populations provide the most robust evidence for fluctuating selection as a mechanism of maintaining genetic diversity due to a lack of long-term observational studies of historical allele-frequency dynamics. However, the existing studies in other species also support the importance of seasonality and fluctuating selection [26]. Hence, theoretical studies of this phenomenon may provide valuable insights that cannot easily be observed experimentally.

Discrete vs. continuous models of periodicity

White and Hastings (2020) describe a variety of methods for modeling seasonality [66]. Models may be discrete, continuous, or incorporate a combination of continuous and discrete elements. Continuous models employ systems of differential equations with parameters which depend on time in a periodic manner. This can be used to model a system with good and bad seasons, such as in the Kremer and Klausmeier model described below [31]. A common strategy for analysing these systems is Floquet theory, which allows for the analysis of stability around a linearised periodic system [29]. Seasonality can also be incorporated into a model based on differential equations by introducing a periodic impulse on the population dynamics. This can be an appropriate way to model a population with continous dynamics but that exists in an environment with discrete seasonality. Another means of combining discrete and continuous dynamics is by considering seasons in discrete time while modelling the growth dynamics within a given season in continuous time [66]. Additionally, models may be entirely discrete, consisting of difference equations such as those used by Roughgarden (1971) [53].

Models of life-history in periodic environments

Kremer and Klausmeier (2013) modeled continuous seasonal fluctuations to show how seasonality can lead to species coexistence [31]. Their model considers an environment which experiences a "growing" season and a "not-growing" season, as represented by a periodically-changing function for resource levels mediating whether or not species experience growth. Seasonality is controlled by two parameters: the total period of the cycle and the proportion

of that period that the good season lasts. They also enforced a trade-off between growth rate (r) and competitive ability (K). This was a species with a high growth rate—hence a high fitness in the good season—but a lower competitive ability and therefore lower fitness in the bad season. They demonstrated how coexistence was determined by the nature of the trade-offs, the speed of evolution, and the length of the period and the proportion of the length of the good season relative to the bad season. Their results also suggested the importance of ecological mechanisms such as immigration [31].

Although Kremer and Klausmeier's model studied species coexistence, the question of competition between species is conceptually the same as competition between asexual clones [71]. Thus, their conclusions may also be applied to the evolution of such a population. In diploid populations, however, mating and the nature of the heterozygote's phenotype must also be taken into consideration. Roughgarden (1971) developed a discrete model of life-history evolution in a diploid population which experienced a season of hibernation [53]. In this case, there is a limitation on the size of the population which can survive the hibernation season. Seasonality led to an increased chance of a polymorphism arising, particularly in moderate environments. Roughgarden also demonstrated the role of the heterozygote's phenotype in maintaing a polymorphism, as patterns of dominance compared to heterozygote advantage or disadvantage changed the environmental conditions under which a stable polymorphism could arise. Analysis of a haploid version of Roughgarden's model can be found in Appendix A.3.

To better understand the relationship between age structure and seasonality, Lion and Gandon (2022) developed a new method for studying life-history evolution of class-structured populations subject to periodic environmental variation [37]. They first defined the life cycle of a class-structured population according to a matrix of the transition rates between classes. These rates were allowed to depend on periodic environmental changes, including extrinsic factors. Under the assumption of weak selection, they derived an equation for the selection gradient averaged over the period. This defines an approximation of the invasion fitness of a mutant in the resident population. Lion and Gandon applied this approach to a host-pathogen model to confirm previous work that indicates that pathogen propagule mortality rates have no effect on evolutionary stable virulence. They also ex-

panded on this to show that in a periodic environment, these mortality rates did have an effect on selection for pathogen virulence [37].

2.2.3 Evolution in noisy environments

Even more prevalent than seasonal, deterministic variations are random variations which are inherent to any system. However, while evolutionary processes will always be subject to some amount of noise, some may be noisier than others and thus less accurately described by deterministic equations.

Noise—or stochasticity—can arise from a variety of different sources. Some of these are intrinsic: changes in allele frequencies are subject to stochasticity via genetic drift and random variation of birth and death rates among individuals results in demographic stochasticity. These intrinsic sources of stochasticity have the greatest influence in smaller populations, as they can average out in larger populations. Stochasticity can also come from extrinsic sources. Variability in the environment can affect allele frequencies and demography [25]. Unlike intrinsic factors, environmental stochasticity can affect small and large populations equally [33]. It should also be noted that observed stochasticity may be a result not of stochasticity in the system, but of stochasticity in measurement errors [33]. Here, we shall focus on environmental stochasticity.

Considering environmental stochasticity through the lens of r- vs. K-selection, Pianka (1970) noted that K-selection strategies predominated in constant environments, while r-selection predominated in more variable environments [51]. The prevalence of K-selection strategies in constant environments is in agreements with early models showing populations with greater competitive abilities prevail in constant environments (see Figure 2.2), however quantifying the observation of r-selection in stochastic environments was more challenging.

Leggett and Carscadden (1978) studied one instance of environmental stochasticity and its relationship to life-history traits in populations of American shad (*Alosa sapidissima*) along the Atlantic coast. They observed that the reproductive strategies of the populations varied with latitude and proposed that this was due to a difference in the amount of environmental stochasticity at different latitudes, as northern environments experience greater variability in water temperatures compared to southern environments [36]. Interestingly, in contrast to simple model predictions, they found that the different reproductive strategy

meant that northern populations had lower fecundity (r) compared to southern populations. This is in opposition to Pianka's observations, as well as the theoretical predictions of Lande *et al.* [34, 35] which will be discussed below. Hence additional explanations, such as bet hedging, may be necessary to fully describe the observed variation in life-history traits of this system.

Long-term evolution in stochastic environments

A consequence of carrying capacity always being maximised by evolution in a constant environment is that changes in the intrinsic growth rate should not have any impact on evolution. An early theoretical study of the relationship between environmental variability and the evolution of growth rate was done by Turelli and Petry (1980) [62]. They considered several discrete-time analogs to the θ-logistic growth equation:

$$\frac{dN}{dt} = r\left[1 - (N/K)^{\theta}\right] N.$$

These analogs took the form:

$$N_{t+1} = G\left[(N/K)^{\theta}; r\right] N_t,$$

where G is a function with r as a parameter. By introducing noise into the function G, they showed that evolution could select for a larger intrinsic growth rate [62].

Lande *et al.* (2009) further explored this idea by deriving a quantity that would be maximised under long-term evolution in a stochastic environment. They considered a general model of density-dependent population growth, then added a white noise term to incorporate environmental stochasticity. When density-dependence takes the form of a θ-logistic growth model, this gives the equation:

$$\frac{dn_i}{dt} = r_i\left[1 - \left(\frac{N}{K_i}\right)^{\theta} + W(t)\right] n_i.$$

Here, $N = \sum_i n_i$ is the total population size, n_i is the number of individuals with the ith genotype, r_i and K_i are the intrinsic growth rate and carrying capacity of the ith genotype respectively, and $W(t)$ is white noise [34]. Using this model, Lande *et al.* concluded that long-

term evolution under logistic growth would maximise the expected long-term population size, given by:

$$\mathrm{E}[N] = (1 - \sigma_e^2/(2r))K^{\theta}, \tag{2.2}$$

where σ_e^2 is a value describing the environmental variance. Equation 2.2 shows that under no constraints, the intrinsic growth rate and carrying capacity should tend toward infinity, while the environmental variance should tend to zero. By introducing a trade-off between r and K, they concluded that for highly variable environments, a larger growth rate is favoured to maximise fitness, while for more constant environments, a higher carrying capacity is favoured. Equation 2.2 also demonstrates that environmental stochasticity decreases average fitness.

Age-structured populations in stochastic environments

It must be noted that fecundity (r) and competitive ability (K) are both traits which vary throughout the life cycle of an organism. For instance, in the life cycle of a typical avian raptor species, both rates of fecundity and of survival will increase through the age classes, and reproduction will only occur upon reaching some age of maturity [35]. Additionally, an organism's contribution and response to density-dependence can change with age. Between different age classes, rates of fecundity and survival may respond more or less strongly to changes in density. Age classes can also contribute differently to population density with changes in their body mass or metabolic rate. In the case of the avian raptor, all age classes experience the same degree of density-dependence on their vital rates. This contrasts with the life cycle of a typical passerine species, where increasing density causes smaller decreases in fecundity as it ages. In both life histories, older individuals contribute more heavily to the overall population density [35]. Age structure can also interact with environmental variance, as the sensitivity of an organism's vital rates to changes in the environment can change throughout its life cycle. Avian raptors show decreasing variability in both rates of fecundity and of survival as they age; in the passerine species the variability of fecundity remains constant throughout the life cycle, while the variability of survival decreases [35].

To better understand how density-dependence, environmental stochasticity, and age structure interact and determine the long-term evolutionary behaviour of a population, Lande *et al.* (2017) developed a model for the growth of a density-dependent age structured population in a stochastic environment. From this they derived a univariate approximation for this growth to find a quantity which is maximised by long-term evolution. Their results showed that incorporating age structure into a model of density-dependent selection on a population in a stochastic environment yields the same conclusion as a model with no age structure. Additionally, their simulations showed that introducing environmental variance reduces the expected population size below the carrying capacity, which provides a mechanism for why a larger growth rate may be favoured in highly variable environments [35].

2.2.4 Examples of environmental variation

Temporal variation in environmental conditions can be found in a plethora of systems. To motivate the study of such variability, I present several examples below.

Tidal disruptions

The seaweed fly *Coelopa frigida* carries a chromosomal inversion which behaves as a single locus with two alleles, α and β [44, 45]. Consequently, *C. frigida* displays three phenotypes: a homozygote with a large body size and slow maturation ($\alpha\alpha$), a homozygote with a small body size and fast maturation ($\beta\beta$), and an intermediate heterozygote ($\alpha\beta$). The habitat of *C. frigida* is subject to periodic disruption by the tide, which causes a spike in mortality of immature flies. While in constant environment experimental conditions, the K-selected $\alpha\alpha$ phenotype is favoured, natural populations subject to these seasonal population crashes contain a much higher proportion of individuals with the more r-selected phenotypes [45].

Winter frost mortality

Winter frosts can also cause seasonal population crashes. The larvae of the yellow dung fly (*Scathophaga stercoraria*) are frost-sensitive and must reach the pupal stage before the frost to survive [60]. Frequent frost events were observed to favour r-selected phenotypes with fast development times. Mortality was higher for large-bodied flies which have slower maturation rates, as they were less likely to reach the pupal stage in time to survive.

Temperature-dependent mortality rates

Seasonal mortality may not always be in the form of sudden deaths, but rather environments can experience seasons of increased mortality and seasons of decreased mortality. One factor that can mediate mortality is temperature. The eastern brook trout (*Salvelinus fontinalis*) experience greater morality among the youngest age class when temperatures rise [4]. This results in higher mortality in the summer, and summer temperatures can have an important impact on population size.

Seasonal predation

Predation patterns can also result in seasonal mortality. This may be due to seasonal patterns in the predator population, or due to changes in coverage protecting prey. For example, in the Caatinga of northwest Sergipe, Brazil, bird attacks increase during the dry season because of the loss of protective cover [14].

Antimicrobial drug regimens

Antimicrobial drug treatments can be periodic in nature, as mortality will increase with each new dose. These periodic environments can change the evolutionary dynamics of populations [69]. Depending on the drug regimen, these disruptions may be discrete, with sudden population crashes each time a dose is delivered, or continuous, with fluctuating drug levels creating periods of high mortality and periods of low mortality.

Precipitation-dependent food availability

Seasonality may also disrupt resource availability. In grasslands, rainfall events influence the quality of vegetation [6]. High-quality vegetation provides more resources for grasshopper populations, leading to reduced density-dependent mortality. Conversely, reduced precipitation causes more density-dependent deaths due to a lack of resources.

Resource fluctuations in chemostat experiments

Resource levels may be varied artificially under experimental conditions. In a chemostat setting, evolution of *Escherichia coli* under alternating periods of feast and famine yielded

populations which maximised rapid growth [65]. Evolution did not lead to reduced death rates or greater capacity for competition for resources.

2.3 Density-dependent selection in spatially-structured environments

2.3.1 Life-history and local adaptation

In addition to varying through time, environmental conditions can vary across space, which may result in local adaptation. Local adaptation is the process by which organisms adapt to their local environment, generally at the cost of reduced fitness in other environments [5]. Not only does this divergent selection across environments play an important role in maintaining biodiversity, it is the first step in the process of ecological speciation [55]. It is also an important factor to consider when a population is expanding its range [3, 16]. Divergent selection is prerequisite for the process of local adaptation; the necessary strength of this selection depends on the extent of the homogenising effects of gene flow between the diverging populations [12, 19, 68, 70]. Although local adaptation has been the topic of extensive study, little is known about the local adaptation of life-history traits.

Gomulkiewicz *et al.* (1999) modelled local adaptation in a sink population sustained by immigration [18]. They incorporated density-dependent effects to show that local adaptation was maximised at intermediate levels of immigration. This was due to the fact that immigration increased density, thus decreasing the overall fitness of the population. The hindering effects of dispersal on local adaptation may be reduced by temporal variations in dispersal rates [50]. This can be observed in the dynamics of pea aphids (*Acyrthosiphon pisum*) and their parasitoid wasp *Aphidius ervi* [46]. However, these results do not speak to the adaptation of density-dependent traits themselves. For this we must look to empirical observations.

Dittmar and Schemske (2023) used reciprocal transplant field experiments and manipulative greenhouse experiments to show that temporal variability mediated the fitness trade-off between strains of the plant *Leptosiphon parviflorus* growing on serpentine soil or non-serpentine soil [12]. In serpentine soil, where water-holding capacity is reduced, *L. parviflorus* has evolved an early-flowering strategy at the cost of competitive ability. This strain

shows a fitness advantage over the native strain in non-serpentine soil in years of low rainfall, but is disadvantaged in years of high rainfall. A similar pattern of local adaptation has been observed in the common yellow monkeyflower, *Mimulus guttatus*: in dry soils, early flowering strategies are favoured, while later flowering and greater competitive ability is favoured at moist, coastal sites [20].

2.3.2 Life-history trade-offs during range expansion

Density-dependent selection and life-history trade-offs are also influenced by spatial structure within the context of range expansion [7, 11, 47, 67]. Deforet *et al.* (2019) demonstrated this in the context of a trade-off between migration and intrinsic growth rate in bacterial colonies [11]. They derived an analytical relationship for how much cost a mutant can incur to its growth rate in favour of higher dispersal before it can no longer invade a resident population. Additionally, they experimentally observed that bacterial populations with higher dispersal consistently out-competed those with higher growth rates. Theoretical work by Burton *et al.* (2010) predicted that evolution will select for higher growth rates and dispersal rates during the expansion of a genetically-heterogeneous population, at the cost of decreased capacity for growth at high densities along the range front [7]. However, simulations also predicted that when the evolving population was forced to compete with a resident population, selection for growth at higher densities increased. Spatial structure can result in a unique stochastic phenomenon known as "allele surfing", where mutations occurring at the outer boundary of a spatially-expanding population can travel along the advancing front and become more likely to reach higher frequencies [22, 23, 30, 61]. Urquhart-Cronish *et al.* (2024) used a one-dimensional stepping-stone simulation to study surfing of life-history traits [63]. They found that surfing of alleles associated with competitive ability was more frequent. Meanwhile, the strong selection for high growth rate along the population edge reduced surfing for that trait. Hall *et al.* (2024) proposed a trade-off between local competitive ability and dispersal to explain the growth behaviour of *Saccharomyces cerevisiae* mats and showed with simulations that although the high dispersing strain showed a fitness advantage in longterm growth, the strain with a high competitive ability was able to consistently take advantage of allele surfing events to temporarily establish mutant segments in a resident population of high dispersers [21].

2.4 Applications to conservation and management

Life-history strategies, local adaptation, and environmental disruptions are all important considerations for conservation efforts in the face of climate change. As the climate changes, environmental disruptions are becoming more frequent: new disruptions arise with increased environmental stochasticity and preexisting disruptive events are becoming more severe and less predictable [13, 56]. A species' life-history will shape how that species responds to such changes, with trends showing that species with faster life history strategies (more r-selected species) adapt more successfully to changing environmental conditions compared to species with slower life history strategies (more K-selected species) [1]. Sæther *et al.* (1996) proposed that life histories could broadly be classified in three categories, based on the quality of the habitats where individuals breed and survive [59]. High-reproductive, or r-selected, species are associated with high-quality breeding habitats but poor-quality habitats for survival. Survivor, or K-selected, species are associated with poor-quality breeding habitats but high-quality habitats for survival. Bet-hedging species are associated with high-quality habitats for both breeding and survival, and have similar survival rates to survivor species, but have greater variance in their reproductive output from season to season. As environments change and species' ranges shift, it's critical to understand how species have adapted to their native habitat and how they may be maladapted to foreign environmental conditions. If a population is highly locally adapted, then a sudden shift in its habitat or a forced shift in its range may be catastrophic. An understanding of how local adaptation has occurred and how future local adaptation in the face of climate change may occur is necessary for successful conservation efforts [42].

Chapter 3

Single-population life-history evolution under seasonal conditions

3.1 Single population model

We begin by considering the evolution of r vs. K life-history traits in a single population. We model population growth with a logistic model where the population size N is given by the differential equation:

$$\frac{dN}{dt} = bN - \left(d + \frac{b}{X}N\right)N,$$

where b is the per-capita birth rate, d is the death rate, and X is the 'growth limit' which determines the carrying capacity (a.k.a. equilibrium) population size K in the long-term:

$$K = \frac{(b-d)X}{b},$$

We additionally note that the intrinsic growth rate of the population is $r = b - d$. To model evolution in this population, we consider the dynamics at a single biallelic, haploid locus with alleles A and a. We choose parameters such that the allele A confers a lower carrying capacity ($K_A < K_a$), but a higher birth rate ($b_A > b_a$). The death rate (d) remains constant across both alleles and must be smaller than both birth rates. Hence we have:

$$0 < d < b_a < b_A,$$
$$\frac{(b_A - d)X_A}{b_A} = K_A < K_a = \frac{(b_a - d)X_a}{b_a}.$$

Therefore, we call the A allele the "high-r" allele and the a allele the "high-K" allele. Evolution is described by a Lotka-Volterra model of competition between individuals carrying the high-r A allele and individuals carrying the high-K a allele, as given by the following system of differential equations:

$$\frac{dN_A}{dt} = b_A N_A - \left(d + \frac{b_A}{X_A}(N_A + N_a)\right) N_A,$$
$$\frac{dN_a}{dt} = b_a N_a - \left(d + \frac{b_a}{X_a}(N_A + N_a)\right) N_a,$$

where N_A is the number of individuals carrying the A allele and N_a is the number with the a allele.

It is convenient to re-parametrise these two equations in terms of the frequency of the A allele, p, and the total population size, N:

$$p = \frac{N_A}{N_A + N_a},$$
$$N = N_A + N_a.$$

Hence changes in the allele frequency and changes in the total population size can be described by the following differential equations:

$$\frac{dp}{dt} = p(1-p)\left(b_A\left(1 - \frac{N}{X_A}\right) - b_a\left(1 - \frac{N}{X_a}\right)\right) = f_1(p, N) \tag{3.1a}$$
$$\frac{dN}{dt} = \left(b_A\left(1 - \frac{N}{X_A}\right)p + b_a\left(1 - \frac{N}{X_a}\right)(1-p) - d\right) N = f_2(p, N). \tag{3.1b}$$

Note that Eq. 3.1a can also be written as,

$$\frac{dp}{dt} = p(1-p)S(N),$$

where $S(N)$ is the selection coefficient given by:

$$S(N) = b_A\left(1 - \frac{N}{X_A}\right) - b_a\left(1 - \frac{N}{X_a}\right). \tag{3.2}$$

System 3.1 exhibits three equilibria:

$$\begin{aligned} \hat{N} &= 0 && \text{(extinction)} \\ \left(\hat{p}, \hat{N}\right) &= \left(1, \frac{(b_A - d)X_A}{b_A}\right) && \text{(fixation)} \\ \left(\hat{p}, \hat{N}\right) &= \left(0, \frac{(b_a - d)X_a}{b_a}\right) && \text{(loss).} \end{aligned}$$

Extinction is unstable when $b_i > d$ (a condition which is assumed to be met throughout). Fixation of the A allele is always unstable, while its loss is always stable. This agrees with classic theory which holds that in a constant environment, the high-K allele will out-compete the high-r allele and drive it to extinction.

3.2 Seasonal population crashes: an impulsive differential equation approach

In order to incorporate seasonal disruptions, we first consider a case where the population undergoes sudden, periodic population crashes. At the end of every season, a proportion δ of the population is removed. The length of the season is arbitrary, as the birth and death rates can be scaled. To maintain consistency across all our models, we choose a season length of 2π. This model can be described by modifying Eqs. 3.1a and 3.1b to get the following set of impulsive differential equations:

$$\begin{aligned} \frac{dp}{dt} &= f_1(p, N), && t \neq 2k\pi, \\ \frac{dN}{dt} &= f_2(p, N), && t \neq 2k\pi, \quad k = 0, 1, 2, \ldots, \\ p(t) = p(t^-), &\quad N(t) = (1 - \delta)\, N(t^-), && t = 2k\pi, \end{aligned}$$

where $p(t^-)$ and $N(t^-)$ are the allele frequency and the population size immediately before the crash. Note that $p(t^-) = p(t)$, so that the population crash does not change the allele frequency in the population. Hence, there is no selective element to the disruptions. This model is a particular case of the more general Lotka-Volterra system with impulses studied by Liu *et al.* (2007), therefore we can apply their general results to derive results more specific to our case. By Theorem 5.1 in [38], there is no positive periodic solution with

coexistence. There are therefore three possible long-term outcomes: extinction, fixation, or loss. By Lemma 2.1 in [38], if:

$$b_a - d < b_A - d < -\frac{1}{2\pi}\ln(1-\delta), \tag{3.3}$$

then the population will go extinct. Otherwise, there are two semi-trivial positive periodic solutions, $\left(0, \hat{N_a}\right)$ and $\left(1, \hat{N_A}\right)$, where where $\hat{N}_i(t)$ is the positive periodic solution to:

$$\begin{aligned} \frac{dN_i}{dt} &= b_i N_i - \left(d + \frac{b_i}{X_i}N\right) N_i, && t \neq 2k\pi, \\ N_i(t) &= (1-\delta)\, N_i(t^-), && t = 2k\pi. \end{aligned}$$

To find the linear stability of each of these solutions we must compute the mean population over a season:

$$\mathbb{E}(\hat{N}_i) = \frac{1}{2\pi}\int_0^{2\pi} \hat{N}_i(t)dt = \frac{X_i}{b_i}\left((b_i - d) + \frac{1}{2\pi}\ln(1-\delta)\right).$$

For the sake of clean notation, we use expectation notation rather than the bar notation generally used to denote the mean. Using Theorem 4.2 from [38], we can see that the $\hat{p} = 0$ case will be linearly stable if:

$$\begin{aligned} b_a - d &> -\frac{1}{2\pi}\ln(1-\delta) \\ b_A - d &< -\frac{1}{2\pi}\ln(1-\delta) + \frac{b_A}{X_A}\mathbb{E}(\hat{N}_i). \end{aligned}$$

Similarly, the $\hat{p} = 1$ case will be linearly stable if:

$$\begin{aligned} b_A - d &> -\frac{1}{2\pi}\ln(1-\delta) \\ b_a - d &< -\frac{1}{2\pi}\ln(1-\delta) + \frac{b_a}{X_a}\mathbb{E}(\hat{N}_i). \end{aligned}$$

By plugging $\mathbb{E}(\hat{N}_i)$ into our stability condition and rearranging, we find that the $\hat{p} = 0$ case is stable if:

$$\delta < 1 - \exp\left[-2\pi(b_a - d)\right]$$
$$\delta < 1 - \exp\left[-2\pi\left(\frac{b_A X_a(b_a - d) - b_a X_A(b_A - d)}{b_A X_a - b_a X_A}\right)\right].$$

The equilibrium solution $\hat{p} = 1$ is stable if:

$$\delta < 1 - \exp\left[-2\pi(b_A - d)\right]$$
$$\delta > 1 - \exp\left[-2\pi\left(\frac{b_A X_a(b_a - d) - b_a X_A(b_A - d)}{b_A X_a - b_a X_A}\right)\right].$$

Given the restrictions on our parameters, we have that the above bounds are restricted to the order:

$$1-\exp\left[-2\pi\left(\frac{b_A X_a(b_a - d) - b_a X_A(b_A - d)}{b_A X_a - b_a X_A}\right)\right] < 1-\exp\left[-2\pi\left(b_a - d\right)\right] < 1-\exp\left[-2\pi\left(b_A - d\right)\right].$$

Hence we find that the $\hat{p} = 1$ case, when the high-r allele overtakes the population, is linearly stable in the range:

$$1 - \exp\left[-2\pi\left(\frac{b_A X_a(b_a - d) - b_a X_A(b_A - d)}{b_A X_a - b_a X_A}\right)\right] < \delta < 1 - \exp\left[-2\pi(b_A - d)\right]. \tag{3.4}$$

If the magnitude of the population crashes is smaller, then the high-K allele will overtake the population. If the population crashes are too large, the population will go extinct.

3.3 Floquet analysis for continuous disruptions

In the following two sections, we will consider continuous seasonal changes. The population dynamics under these conditions can be described by a small, periodic perturbation to the original system described by Eqs. 3.1a and 3.1b:

$$\frac{dp}{dt} = f_1(p, N) - \epsilon g_1(p, N)$$
$$\frac{dN}{dt} = f_2(p, N) - \epsilon g_2(p, N),$$

where ϵ is a small, positive perturbation and $g_i(p, N)$ are periodic functions. By incorporating any periodic perturbation, the system will no longer reach a constant equilibrium. Rather, we must consider the periodic equilibrium solutions and their stability. To do so, we apply Floquet analysis [29].

Let $\left(\hat{p}, \hat{N}\right)$ be a periodic solution. Then we consider the behaviour of a small perturbation to this solution: $(p(t), N(t)) = \left(\hat{p} + \xi_1(t), \hat{N} + \xi_2(t)\right)$. These perturbations may be written as:

$$\begin{pmatrix} \xi_1(t) \\ \xi_2(t) \end{pmatrix} = \mathbf{\Phi}(t) \begin{pmatrix} \xi_1(0) \\ \xi_2(0) \end{pmatrix},$$

where $\mathbf{\Phi}(t)$ is the matrix satisfying:

$$\frac{d\mathbf{\Phi}}{dt} = \mathbf{A}|_{p=\hat{p}, N=\hat{N}}\, \mathbf{\Phi}(t), \quad \mathbf{\Phi}(0) = \mathbf{I},$$

and $\mathbf{A}$ is the matrix:

$$\mathbf{A} = \begin{pmatrix} \frac{\partial}{\partial p}\left(f_1(p, N) - \epsilon g_1(p, N)\right) & \frac{\partial}{\partial N}\left(f_1(p, N) - \epsilon g_1(p, N)\right) \\ \frac{\partial}{\partial p}\left(f_2(p, N) - \epsilon g_2(p, N)\right) & \frac{\partial}{\partial N}\left(f_2(p, N) - \epsilon g_2(p, N)\right) \end{pmatrix}.$$

Then the Floquet multipliers, ρ_i, of the system are the eigenvalues of $\mathbf{\Phi}(2\pi)$. The periodic solution $\left(\hat{p}, \hat{N}\right)$ is locally stable if both of its Floquet multipliers satisfy:

$$|\rho_i| < 1.$$

In some cases, it may be easier to look at the Floquet exponents, λ_i, which are derived from the Floquet multipliers by:

$$\lambda_i = \frac{1}{2\pi} \ln |\rho_i|.$$

In order for the periodic solution to be locally stable, these Floquet exponents must be negative.

3.4 Continuous seasonal variations in death rates

To model continuous variation in the death rate, we substitute $d \mapsto d\,(1 + \epsilon h(t))$, where $h(t)$ is a periodic function and $\epsilon \in (0, 1)$ is a small quantity. This restriction of ϵ indicates that we are considering a death rate that depends weakly on time and ensures that the death rate is always positive. Without loss of generality, we may assume that $h(t)$ has a period of 2π. For longer or shorter seasons, the birth and death rates can be scaled. This results in the perturbed problem:

$$\begin{aligned}\frac{dp}{dt} &= f_1(p, N)\\ \frac{dN}{dt} &= f_2(p, N) - \epsilon d N h(t).\end{aligned}$$

We could consider a specific periodic function $h(t)$, but as we will show below, the result is sensitive to the shape of this function. Hence we take a general approach where we express $h(t)$ as a Fourier series:

$$h(t) = A_0 + \sum_{n=1}^{\infty} A_n \cos nt + B_n \sin nt,$$

where:

$$\begin{aligned}A_0 &= \frac{1}{2\pi}\int_0^{2\pi} h(t)dt,\\ A_n &= \frac{1}{\pi}\int_0^{2\pi} h(t)\cos(nt)dt,\\ B_n &= \frac{1}{\pi}\int_0^{2\pi} h(t)\sin(nt)dt.\end{aligned}$$

The Floquet exponents for this system are:

$$\lambda_1 = \frac{1}{2\pi}\int_0^{2\pi} \frac{\partial}{\partial N} f_2(p(t), N(t)) - \epsilon d h(t)dt \tag{3.5}$$

$$\lambda_2 = \frac{1}{2\pi}\int_0^{2\pi} (1 - 2p(t))\, S\,(N(t))\, dt, \tag{3.6}$$

where $S(N)$ is the selection coefficient given in Eq. 3.2. We seek that Eqs. 3.5 and 3.6 be negative to ensure the local stability of the solution.

We first check the stability conditions for the equilibrium states when the population goes extinct, $\left(\hat{p}, \hat{N}\right) = (0, 0)$ and $\left(\hat{p}, \hat{N}\right) = (1, 0)$. Given $b_A > b_a$, we find Eq. 3.6 is always positive for $\left(\hat{p}, \hat{N}\right) = (0, 0)$, so this state is always unstable. For $\left(\hat{p}, \hat{N}\right) = (1, 0)$, Eq. 3.6 is always negative. From Eq. 3.5 we find that the condition for $\left(\hat{p}, \hat{N}\right) = (1, 0)$ to be stable is:

$$\epsilon A_0 > \frac{b_A}{d} - 1.$$

This is our condition for extinction.

To determine which genotype will dominate when the population is not driven to extinction, we first consider the equilibrium at $\hat{p} = 0$, when the r-selected A allele is lost. Recall that in the unperturbed problem, this is always the stable steady state. To consider the periodic equilibrium solution for the population size in this case, we take the asymptotic expansion:

$$\hat{N} = N_0 + \epsilon N_1 + \mathcal{O}(\epsilon^2),$$

and plug this into the perturbed equation for population size:

$$\frac{dN}{dt} = \left(b_a \left(1 - \frac{N}{X_a}\right) - d\right) N - \epsilon d h(t) N.$$

At $\mathcal{O}(1)$, we arrive at the unperturbed problem. We take the leading order of our expansion to be the stable steady state, so:

$$N_0 = \frac{(b_a - d) X_a}{b_a}.$$

At $\mathcal{O}(\epsilon)$, we get the differential equation:

$$\frac{dN_1}{dt} = -(b_a - d) N_1 - d N_0 \left[A_0 + \sum_{n=1}^{\infty} \left(A_n \cos nt + B_n \sin nt\right)\right]. \tag{3.7}$$

Since we are looking for a periodic solution, we assume that N_1 can be written as a Fourier series:

$$N_1(t) = a_0 + \sum_{n=1}^{\infty} \left(a_n \cos nt + b_n \sin nt\right).$$

Plugging this into Eq. 3.7 and taking $\alpha = -(b_a - d)$ and $\beta = dN_0$, we find that:

$$\alpha a_0 - \beta A_0 + \sum_{n=1}^{\infty} \left((\alpha a_n - \beta A_n - n b_n) \cos nt + (\alpha b_n - \beta B_n + n a_n) \sin nt \right) = 0.$$

This implies that:

$$\begin{aligned} \alpha a_0 - \beta A_0 &= 0, \\ \alpha a_n - \beta A_n - n b_a &= 0, \\ \alpha b_n - \beta B_n + n a_n &= 0, \end{aligned}$$

hence:

$$\begin{aligned} a_0 &= \frac{\beta}{\alpha} A_0, \\ a_n &= \frac{\beta \left(\alpha A_n + n B_n \right)}{\alpha^2 + n^2}, \\ b_n &= \frac{\beta \left(\alpha B_n - n A_n \right)}{\alpha^2 + n^2}. \end{aligned}$$

Therefore:

$$N_1 = \frac{\beta}{\alpha} A_0 + \sum_{n=1}^{\infty} \left(\frac{\beta \left(\alpha A_n + n B_n \right)}{\alpha^2 + n^2} \cos nt + \frac{\beta \left(\alpha B_n - n A_n \right)}{\alpha^2 + n^2} \sin nt \right),$$

which gives us the asymptotic expansion of $\hat{N}$ near the steady state of the unperturbed problem:

$$\hat{N} = N_0 + \epsilon \left[\frac{\beta}{\alpha} A_0 + \sum_{n=1}^{\infty} \left(\frac{\beta \left(\alpha A_n + n B_n \right)}{\alpha^2 + n^2} \cos nt + \frac{\beta \left(\alpha B_n - n A_n \right)}{\alpha^2 + n^2} \sin nt \right) \right] + \mathcal{O}(\epsilon^2).$$

Plugging $\hat{p} = 0$ into our first Floquet exponent (Eq. 3.5), we have:

$$\lambda_1 = \frac{1}{2\pi} \int_0^{2\pi} b_a - d - \frac{2 b_a}{X_a} \hat{N}(t) - \epsilon d h(t) dt.$$

This requires us to compute:

$$\begin{aligned}\int_0^{2\pi} \hat{N} &= \int_0^{2\pi} N_0 + \epsilon \left[\frac{\beta}{\alpha} A_0 + \sum_{n=1}^{\infty} (a_n \cos nt + b_n \sin nt)\right] dt \\ &= 2\pi \left(N_0 + \epsilon \frac{\beta}{\alpha} A_0\right) + \epsilon \sum_{n=1}^{\infty} \left(a_n \int_0^{2\pi} \cos(nt) dt + b_n \int_0^{2\pi} \sin(nt) dt\right) \\ &= 2\pi \left(N_0 + \epsilon \frac{\beta}{\alpha} A_0\right).\end{aligned} \tag{3.8}$$

Plugging Eq. 3.8 into our Floquet exponent and recalling that $A_0 = \frac{1}{2\pi} \int_0^{2\pi} h(t) dt$, we find that:

$$\lambda_1 = -\left[b_a - d(1 + \epsilon A_0)\right].$$

This is negative so long as:

$$\epsilon A_0 < \frac{b_a}{d} - 1.$$

It remains to check whether the direction of selection will change due to the seasonal perturbation. We therefore check the second Floquet exponent (Eq. 3.6). Substituting $\alpha = -(b_a - d)$ and $\beta = dN_0$ back in and using the result in Eq. 3.8, we find that the second exponent is negative when the following inequality holds:

$$\epsilon A_0 < \frac{b_A X_a (b_a - d) - b_a X_A (b_A - d)}{d(b_A X_a - b_a X_A)}. \tag{3.9}$$

Since:

$$\frac{b_A X_a (b_a - d) - b_a X_A (b_A - d)}{d(b_A X_a - b_a X_A)} < \frac{b_a}{d} - 1,$$

we see that $\hat{p} = 0$ is stable whenever Eq. 3.9 holds.

To consider the stability of $\hat{p} = 1$, we follow the same steps and find that the first Floquet exponent (Eq. 3.5) is negative when:

$$\epsilon A_0 < \frac{b_A}{d} - 1,$$

and the second Floquet exponent (Eq. 3.6) is negative when Eq. 3.9 does not hold. Since:

$$\frac{b_A X_a (b_a - d) - b_a X_A (b_A - d)}{d(b_A X_a - b_a X_A)} < \frac{b_A}{d} - 1,$$

the $\hat{p} = 1$ solution is stable when ϵA_0 is between these two values. Thus, the high-r allele will dominate the population when:

$$\frac{b_A X_a (b_a - d) - b_a X_A (b_A - d)}{d(b_A X_a - b_a X_A)} < \epsilon A_0 < \frac{b_A}{d} - 1. \tag{3.10}$$

In this case, the seasonal perturbations to the death rate are large enough and long enough to favour high-r strategies, but not so harsh that the population is driven extinct. Note that as the baseline death rate, d, increases, this window for ϵA_0 shifts so that seasonal perturbations need not be as harsh. We also note that Eq. 3.10 can equivalently be written as:

$$1 - \exp\left[-2\pi\left(\frac{b_A X_a (b_a - d) - b_a X_A (b_A - d)}{b_A X_a - b_a X_A}\right)\right] < 1 - e^{-2\pi d\epsilon A_0} < 1 - \exp\left[-2\pi(b_A - d)\right],$$

which is the same inequality as Eq. 3.4, except with δ replaced by $1 - e^{-2\pi d\epsilon A_0}$. This is the probability of there being a death in 2π time in a Poisson process with a death rate of $d\epsilon A_0$. Given that $d\epsilon A_0$ is the averaged size of the perturbation to the death rate, this can be interpreted as the proportion of the population killed due to the perturbed death rate. Hence δ and $1 - e^{-2\pi d\epsilon A_0}$ both represent the proportion of the population that dies over the course of the season above what would be expected from the natural death rate.

3.5 Continuous seasonal variations in resource levels

To model continuous variation in the resource levels, we apply a periodic change to the carrying capacity by substituting $X_i^{-1} \mapsto X_i^{-1}(1 + \epsilon h(t))$, where $h(t)$ is a periodic function. Without loss of generality, we again assume that $h(t)$ has a period of 2π. Rewriting our functions, we arrive at the perturbed problem:

$$\begin{aligned}
\frac{dp}{dt} &= f_1(p, N) - \epsilon p(1-p)\left(\frac{b_A}{X_A} - \frac{b_a}{X_a}\right) N h(t) \\
\frac{dN}{dt} &= f_2(p, N) - \epsilon\left[p\frac{b_A}{X_A} - (1-p)\frac{b_a}{X_a}\right] N^2 h(t).
\end{aligned}$$

We express $h(t)$ as a Fourier series as before. Recall that from this we have:

$$A_0 = \frac{1}{2\pi}\int_0^{2\pi} h(t)dt.$$

Now the Floquet exponents for this system are:

$$\lambda_1 = \frac{1}{2\pi}\int_0^{2\pi} \frac{\partial}{\partial N} f_2(p(t), N(t)) - \epsilon\left(2\frac{b_A}{X_A}p(t) - 2\frac{b_a}{X_a}(1-p(t))\right)N(t)h(t)dt, \tag{3.11}$$

$$\lambda_2 = \frac{1}{2\pi}\int_0^{2\pi} (1-2p(t))S(N(t)) - \epsilon(1-2p(t))\left(\frac{b_A}{X_A} - \frac{b_a}{X_a}\right)N(t)h(t)dt. \tag{3.12}$$

These must be negative to ensure local stability.

We first check the extinction cases: $\left(\hat{p}, \hat{N}\right) = (0,0)$ and $\left(\hat{p}, \hat{N}\right) = (1,0)$. Given $b_A > b_a > d$, Eq. 3.11 is always positive for both extinction cases. Therefore, seasonal perturbations to the resource levels cannot drive the population extinct.

We next consider the equilibrium at $\hat{p} = 0$ when the r-selected A allele is lost. In the unperturbed problem, this is always the stable steady state. Once again, we take the asymptotic expansion of $\hat{N}(t)$ and plug this into the perturbed equation for population size:

$$\frac{dN}{dt} = \left(b_a\left(1 - \frac{N}{X_a}\right) - d\right)N - \epsilon\frac{b_a}{X_a}h(t)N.$$

At $\mathcal{O}(1)$, we have the unperturbed problem and take the leading order of our expansion to be its stable steady state. At $\mathcal{O}(\epsilon)$, we get the differential equation:

$$\frac{dN_1}{dt} = \left(b_a - d - 2\frac{b_a}{X_a}N_0\right)N_1 - \frac{b_a}{X_a}N_0\left[A_0 + \sum_{n=1}^{\infty}\left(A_n\cos nt + B_n\sin nt\right)\right]. \tag{3.13}$$

Since we are looking for a periodic solution, we again require that N_1 can be written as a Fourier series:

$$N_1(t) = a_0 + \sum_{n=1}^{\infty} a_n\cos nt + b_n\sin nt.$$

Plugging this into Eq. 3.13 and taking $\alpha = -\left(b_a - d\right)$ and $\beta = (b_a - d)N_0$, we find that:

$$\alpha a_0 - \beta A_0 + \sum_{n=1}^{\infty}\left(\left(\alpha a_n - \beta A_n - nb_n\right)\cos nt + \left(\alpha b_n - \beta B_n + na_n\right)\sin nt\right) = 0.$$

This implies that:

$$\begin{aligned}
\alpha a_0 - \beta A_0 &= 0, \\
\alpha a_n - \beta A_n - n b_n &= 0, \\
\alpha b_n - \beta B_n + n a_n &= 0,
\end{aligned}$$

hence:

$$\begin{aligned}
a_0 &= \frac{\beta}{\alpha} A_0, \\
a_n &= \frac{\beta\left(\alpha A_n + n B_n\right)}{\alpha^2 + n^2}, \\
b_n &= \frac{\beta\left(\alpha B_n - n A_n\right)}{\alpha^2 + n^2}.
\end{aligned}$$

Altogether, we have the asymptotic expansion of $\hat{N}$ near the steady state of the unperturbed problem:

$$\hat{N} = N_0 + \epsilon\left[\frac{\beta}{\alpha} A_0 + \sum_{n=1}^{\infty}\left(\frac{\beta\left(\alpha A_n + n B_n\right)}{\alpha^2 + n^2}\cos nt + \frac{\beta\left(\alpha B_n - n A_n\right)}{\alpha^2 + n^2}\sin nt\right)\right] + \mathcal{O}(\epsilon^2).$$

The integral of this is the same as in Eq. 3.8 from the previous case.

We now plug $\hat{p} = 0$ and $\hat{N}$ into our first Floquet exponent (Eq. 3.11). Dropping all terms that are $\mathcal{O}(\epsilon^2)$ or smaller and using Eq. 3.8, we get:

$$\begin{aligned}
\lambda_1 &= \frac{1}{2\pi}\int_0^{2\pi} b_a - d - 2\frac{b_a}{X_a}\hat{N} + \epsilon\left(2\frac{b_a}{X_a} N_0 h(t)\right) dt \\
&= -\left(b_a - d\right),
\end{aligned}$$

which is always negative as we have already required that $d < b_a$.

Similarly for the second Floquet exponent (Eq. 3.12), we find that:

$$\begin{aligned}
\lambda_2 &= \frac{1}{2\pi}\int_0^{2\pi} b_A - b_a\left(\frac{b_A}{X_A} - \frac{b_a}{X_a}\right)\hat{N} - \epsilon\left(\frac{b_A}{X_A} - \frac{b_a}{X_a}\right) N_0 h(t) dt \\
&= \left(b_A - b_a\left(\frac{b_A}{X_A}\right) N_0\right) \\
&= \left(S(N_0)\right),
\end{aligned}$$

$$\frac{dN_i}{dt} = b_i N_i - \left(d + \frac{N}{X_i}\right) N_i$$
$$N_i(t) = (1-\delta) N_i(t^-)$$

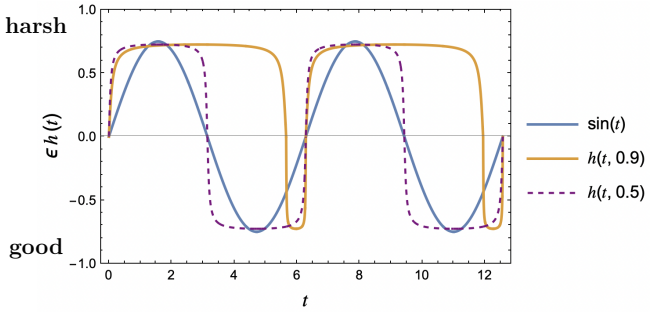

Model	Trait	Condition for r-selection
Impulsive	$\delta > 0$	$1 - \exp[-2\pi C] < \delta < 1 - \exp[-2\pi(b_A - d)]$
Continuous	$d \mapsto d(1 + \epsilon h(t))$	$1 - \exp[-2\pi C] < 1 - e^{-2\pi d \epsilon A_0} < 1 - \exp[-2\pi(b_A - d)]$
Continuous	$X_i^{-1} \mapsto X_i^{-1}(1 + \epsilon h(t))$	None

$$C = \frac{b_A X_a (b_a - d) - b_a X_A (b_A - d)}{b_A X_a - b_a X_A} \qquad A_0 = \frac{1}{2\pi} \int_0^{2\pi} h(t) dt$$

Figure 3.1: **Summary of single population results.** The general model (top left) can be varied according to three different traits: the proportion of individuals removed from the population at the end of a season (δ); the death rate (d); and the growth limit, or resources available (X_i). The death rate and growth limit are varied seasonally by incorporating a periodic function, $\epsilon h(t)$, which creates seasons with good conditions and seasons with harsh conditions. Example functions are shown in the top right.

where $S(N)$ is the selection coefficient in the unperturbed environment (Eq. 3.2). Since we have chosen our parameters to favour the a allele in the unperturbed environment, we know this value to be negative. Thus we find that the equilibrium at $\hat{p} = 0$ is locally stable regardless of any perturbation to the environment. Carrying out a similar analysis for the $\hat{p} = 1$ case, we find that this case is always locally unstable. Therefore, we conclude that a perturbation to resource levels in the environment cannot change the evolutionary outcome.

Chapter 4

Local adaptation to seasonal population crashes

4.1 Island-mainland model

To study adaptation of a population to local seasonal disruptions, we consider an island-mainland model where the environment is constant on the mainland and seasonal on the island. Migration is unidirectional from the mainland to the island. As before, we consider the evolution of r vs. K life-history strategies determined by a single, haploid, biallelic locus. Under these assumptions the mainland will consist entirely of high-K (a allele) individuals. Assuming logistic population growth, the eco-evolutionary dynamics on the island is given by a system of differential equations for the densities of the high-r, A allele (N_A) and the high-K, a allele (N_a). Migration from the mainland introduces a alleles at a constant rate M:

$$\begin{aligned}\frac{dN_A}{dt} &= b_A N_A - \left(d + \frac{N_A + N_a}{X_A}\right) N_A, \\ \frac{dN_a}{dt} &= b_a N_a - \left(d + \frac{N_A + N_a}{X_a}\right) N_a + M.\end{aligned}$$

As before, we perform a change of variables rewriting this system in terms of the frequency of the high-r A allele on the island (p) and the total population size (N) on the island:

$$\frac{dp}{dt} = p(1-p)\left(b_A\left(1 - \frac{N}{X_A}\right) - b_a\left(1 - \frac{N}{X_a}\right)\right) - p\frac{M}{N} = \tilde{f}_1(p, N) \tag{4.1}$$

$$\frac{dN}{dt} = \left(b_A\left(1 - \frac{N}{X_A}\right)p + b_a\left(1 - \frac{N}{X_a}\right)(1-p) - d\right)N + M = \tilde{f}_2(p, N). \tag{4.2}$$

As in section 3.2, we incorporate seasonality by including periodic population crashes where every 2π units of time the population density is reduced by a proportion δ. These population crashes are non-selective, with individuals removed at random such that the allele frequency remains unchanged. Hence, our island is modelled by the set of impulsive differential equations:

$$\begin{aligned}
\frac{dp}{dt} &= \tilde{f}_1(p,N), && t \neq 2k\pi, \\
\frac{dN}{dt} &= \tilde{f}_2(p,N), && t \neq 2k\pi, \quad k = 0,1,2,\ldots, \\
p(t) &= p(t^-), \quad N(t) = (1-\delta)\,N(t^-), && t = 2k\pi.
\end{aligned}$$

In contrast to the single population model, the constant influx of a alleles means that the a allele can never go extinct on the island. Hence, there are only two possible long-term evolutionary outcomes. Either the A allele goes extinct so that $\hat{p} = 0$, or a polymorphism arises on the island where the two alleles coexist.

4.2 Floquet analysis

We again apply Floquet analysis [29] to study the stability of the periodic solution when $\hat{p} = 0$. In the long-term, this periodic solution must consist of repeated cycles where the population size grows logistically from an initial size to some maximum immediately before the crash. To obtain an identical cycle in the next time interval, the population must crash down to the same initial density as at the beginning of the cycle. Hence we can solve for this periodic solution by solving for the general solution from time $0 \leq t \leq 2\pi$ and then solving for the initial condition N_0 that results in the required limit cycle. In this case, $\hat{N}(t)$ is the solution to:

$$\frac{dN}{dt} = b_a N - \left(d + \frac{N}{X_a}\right) N + M, \quad 0 \leq t \leq 2\pi, \quad N(0) = (1-\delta)N(2\pi),$$

which is given by:

$$\hat{N}(t) = \frac{C_2 N_0 \left(1 + e^{C_1 t}\right) - \left(2M + (b_a - d)N_0\right) X_a \left(1 - e^{C_1 t}\right)}{C_2 \left(1 + e^{C_1 t}\right) - \left(2b_a N_0 - X_a(b_a - d)\right)\left(1 - e^{C_1 t}\right)},$$

where:

$$C_1 = \frac{\sqrt{4b_aM + (b_a - d)^2 X_a}}{\sqrt{X_a}},$$
$$C_2 = \sqrt{X_a}\sqrt{4b_aM + (b_a - d)^2 X_a},$$

and N_0 is such that:

$$N_0 = \hat{N}(0) = (1 - \delta)\hat{N}(2\pi),$$

that is:

$$N_0 = \frac{X_a}{2}\left(1 - \frac{d}{b_a}\right)\left(1 - \frac{\delta}{2}\right) - \frac{C_3}{4b_aC_4} + \frac{\sqrt{4(1-\delta)b_aX_aMC_4^2 + \frac{1}{4}\left((b_a - d)X_aC_4(-2 + \delta) + \delta C_2C_3\right)^2}}{2b_aC_4},$$

where:

$$C_3 = e^{C_1\pi} + e^{-C_1\pi},$$
$$C_4 = e^{C_1\pi} - e^{-C_1\pi}.$$

This is non-negative only if $C_2 \in \mathbb{R}$ and $e^{C_1\pi} > 1$. If $C_2 \in \mathbb{R}$, then C_1 must also be real and positive, hence $e^{C_1\pi} > 1$ is automatically true and we need only check $C_2 \in \mathbb{R}$. This is true if:

$$4b_aM + (b_a - d)^2 X_a \geq 0,$$

which is clearly true. Thus $\hat{N}$ is a biologically-viable solution.

As before (sec. 3.3), to study the stability of a periodic solution $\left(\hat{p}, \hat{N}\right)$, we consider the behaviour of a small perturbation to the solution: $(p(t), N(t)) = \left(\hat{p} + \xi_1(t), \hat{N} + \xi_2(t)\right)$. These perturbations may be written as:

$$\begin{pmatrix} \xi_1(t) \\ \xi_2(t) \end{pmatrix} = \mathbf{\Phi}(t) \begin{pmatrix} \xi_1(0) \\ \xi_2(0) \end{pmatrix},$$

where $\mathbf{\Phi}(t)$ is the matrix satisfying:

$$\frac{d\mathbf{\Phi}}{dt} = \left.\begin{pmatrix} \frac{\partial}{\partial p}\tilde{f}_1(p,N) & \frac{\partial}{\partial N}\tilde{f}_1(p,N) \\ \frac{\partial}{\partial p}\tilde{f}_2(p,N) & \frac{\partial}{\partial N}\tilde{f}_2(p,N) \end{pmatrix}\right|_{p=\hat{p},N=\hat{N}} \mathbf{\Phi}(t), \quad t \neq 2k\pi, \quad k = 0,1,2,\ldots, \quad \mathbf{\Phi}(0) = \mathbf{I}.$$

The effect of our impulsive condition is given by:

$$\begin{pmatrix} \xi_1(2\pi) \\ \xi_2(2\pi) \end{pmatrix} = \begin{pmatrix} 1 & 0 \\ 0 & 1-\delta \end{pmatrix} \begin{pmatrix} \xi_1(2\pi^-) \\ \xi_2(2\pi^-) \end{pmatrix},$$

hence Floquet multipliers are the eigenvalues of:

$$M = \begin{pmatrix} 1 & 0 \\ 0 & 1-\delta \end{pmatrix} \mathbf{\Phi}(2\pi).$$

Solving this for the $\hat{p} = 0$ solution, we get the two Floquet multipliers:

$$\rho_1 = \exp\left[\int_0^{2\pi} \left(b_A\left(1 - \frac{\hat{N}}{X_A}\right) - b_a\left(1 - \frac{\hat{N}}{X_a}\right) - \frac{M}{\hat{N}}\right) dt\right]$$
$$\rho_2 = (1-\delta)\exp\left[\int_0^{2\pi} \left(b_a\left(1 - 2\frac{\hat{N}}{X_a}\right) - d\right) dt\right].$$

Numerically, we see that ρ_2 is always less than 1, hence we need only check when $\rho_1 < 1$ for stability (see Mathematica file for details). The first Floquet multiplier is less than one only if the associated Floquet exponent is negative, where the exponent is given by:

$$\lambda_1 = \frac{1}{2\pi}\int_0^{2\pi} \left(b_A\left(1 - \frac{\hat{N}}{X_A}\right) - b_a\left(1 - \frac{\hat{N}}{X_a}\right) - \frac{M}{\hat{N}}\right) dt. \tag{4.3}$$

We calculate this value numerically across a range of parameter values (see Mathematica file for details) and compare the stability results of the island-mainland case to the minimum degree of environmental harshness (δ) needed for selection to favour the high-r, a allele in the single population case (Eq. 3.4). We call this value the coexistence criterion, as δ must at least be greater than this criterion in order for coexistence to occur. Fig. 4.1A shows that this criterion is not sufficient for coexistence to occur; for smaller carrying capacities, environmental harshness must be a good deal greater due to the constant migration

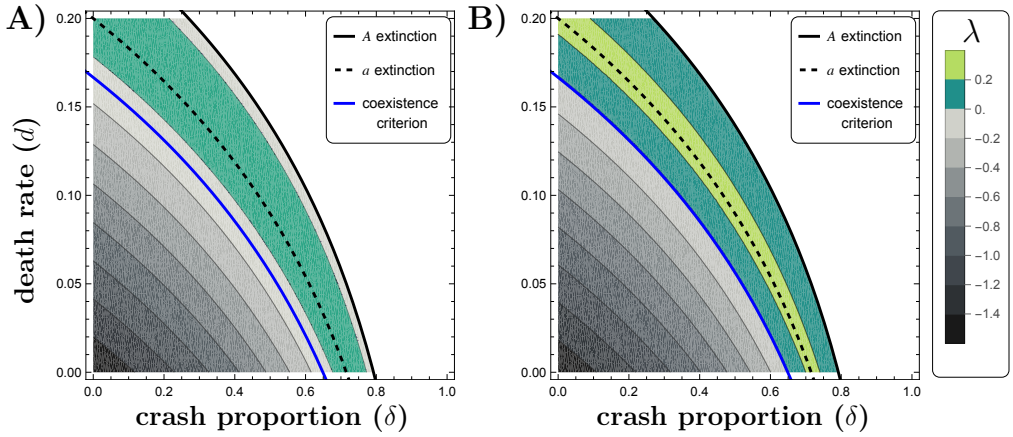

Figure 4.1: **Stability of $\hat{p}(t) = 0$ under different environmental conditions.** Stability is given by the sign of λ in Eq. 4.3. When $\lambda < 0$ (grey), then $\hat{p}(t) = 0$ is stable, hence the high-r A allele is driven to extinction on the island and no local adaptation occurs. When $\lambda > 0$ (turquoise), then $\hat{p}(t) = 0$ is unstable, hence the A allele persists and the island population is locally adapted relative to the mainland. Stability was calculated across different degrees of environmental harshness (δ) and baseline death rates (d). The death rate was allowed to range from 0 to b_a. For a given d, δ values were chosen to be below the A extinction criterion (black line), the maximum δ such that a single population of A allele individuals is still viable (Eq. 3.3). Above this value (white region), the island population is a sink sustained only by migration from the mainland. A similar extinction criterion for the a allele is indicated by the dotted line (Eq. 3.3), indicating the maximum δ such that a single population of a allele individuals would be viable. The blue line marks the minimum value of δ required for selection to favour the high-r allele in the single population case, as given by Eq. 3.4. Parameters were as follows: (A) $b_A = 0.25$, $b_a = 0.2$, $X_A = 500$, $X_a = 1000$, $M = 1$; (B) $b_A = 0.25$, $b_a = 0.2$, $X_A = 5000$, $X_a = 10000$, $M = 1$.

of new individuals increasing the overall island population size, thus requiring a harsher environment to reduce the population sufficiently to favour the high-r allele. We also note that if the environment is too harsh, the high-K individuals migrating in will out-compete the dwindling high-r individuals, even before the environment is sufficiently harsh to drive the high-r alleles to extinction entirely. Thus the window in which a polymorphism persists and the island becomes locally adapted to favour the high-r allele may be smaller than the window in which the high-r allele is favoured in a single population model. As carrying capacity increases (Fig. 4.1B), the parameter region in which coexistence occurs grows to match the parameter region in which the high-r allele dominates in the single-population model.

4.3 Estimating the polymorphic solution

When $\hat{p} = 0$ is not stable, coexistence of the two alleles arises so that $0 < \hat{p} < 1$. Since $p(t) = p(t^-)$, a long term periodic solution requires that the allele frequency at the beginning of the season is equal to the allele frequency at the end of the season. Therefore we assume the change in allele frequency throughout the season is small, hence:

$$\frac{dp}{dt} \approx 0.$$

Setting Eq. 4.1 equal to zero, we find:

$$p(N(t)) = \frac{b_A X_a N(N - X_A) - b_a X_A N(N - X_a) + X_A X_a M}{b_A X_a N(N - X_A) - b_a X_A N(N - X_a)}.$$

Plugging this in for p, Eq. 4.2 reduces to:

$$\frac{dN}{dt} = b_A N - \left(d + \frac{b_A}{X_A} N\right) N,$$

which along with our impulse restriction gives us the approximate periodic solution:

$$\hat{N}(t) = \frac{(b_A - d)X_A}{b_A} \frac{e^{-2\pi(b_A - d)} - (1 - \delta)}{e^{-2\pi(b_A - d)} - (1 - \delta) - \delta e^{-(b_A - d)t}}.$$

Plugging this into Eq. 4.1, we get the following differential equation:

$$\frac{dp}{dt} = a_1(t)p + a_2(t)p^2,$$

where:

$$\begin{aligned} a_1(t) = (b_A - b_a) - \frac{b_A M}{(b_A - d)X_A} + \frac{b_A M \delta e^{-(b_A - d)t}}{(b_A - d)X_A \left(e^{-2\pi(b_A - d)} - (1 - \delta)\right)} \\ - \frac{(b_A - d)(b_A X_a - b_a X_A)\left(e^{-2\pi(b_A - d)} - (1 - \delta\right)}{b_A X_A \left(e^{-2\pi(b_A - d)} - (1 - \delta) - \delta e^{-(b_A - d)t}\right)}, \\ a_2(t) = -(b_A - b_a) + \frac{(b_A - d)(b_A X_a - b_a X_A)\left(e^{-2\pi(b_A - d)} - (1 - \delta\right)}{b_A X_A \left(e^{-2\pi(b_A - d)} - (1 - \delta) - \delta e^{-(b_A - d)t}\right)}. \end{aligned}$$

Using the change of variables [64]:

$$p(t) = -\frac{y'(t)}{a_2(t)y(t)}, \quad y'(0) = -a_2(0)p(0), \quad y(0) = 1,$$

we derive an approximate long-term periodic solution $\hat{p}(t)$ for the polymorphic state:

$$\hat{p}(t) = \frac{Cb(t)}{1 - C\int_0^t a_2(s)b(s)ds},$$

where:

$$b(t) = \exp\left[\int a_1(t)\right]$$
$$C = -\frac{\hat{p}(0)}{b(0)}.$$

To satisfy the requirements of a periodic solution, we require that $\hat{p}(0) = \hat{p}(2\pi)$ so that:

$$\hat{p}(0) = \frac{b(0) - b(2\pi)}{\int_0^{2\pi} a_2(s)b(s)ds}.$$

This solution cannot be written in closed form and must be computed numerically.

4.4 Calculating local adaptation

While the stability analysis informs when coexistence occurs, it does not describe the extent of local adaptation on the island. In the case that the A allele persists, the extent of local adaptation can be quantified using the 'local vs. foreign' definition of local adaptation [5]:

$$\Delta_{LF} = \mathbb{E}[W_{ii}] - \mathbb{E}_j[W_{ij}],$$

which takes the difference between the mean fitness of island (i) individuals in the island (i) environment and the mean fitness of all individuals from all populations ($j = \{$island, mainland$\}$) when transplanted into the home (island) environment [27]. In the case of the island-mainland model, this becomes:

$$\Delta_{LF} = \frac{1}{2}\left(pW_A + (1-p)\,W_a\right) - \frac{1}{2}W_a. \tag{4.4}$$

Here the fitness of an allele is given by:

$$W_i = b_i - \left(d + \frac{b_i}{X_i} N \right).$$

Since fitness is dependent on the population density in the environment (N) and allele frequency (p), which both change with time, it is necessary to choose a time when local adaptation will be measured. We choose to measure the degree of local adaptation on the island at both the beginning of the season and at the end, just before the crash.

Figure 4.2 shows how locally adapted the island is under different environmental conditions. At the beginning of the season, the island is always positively locally adapted, but by the end of the season, the degree of local adaptation has decreased across all environments. When the island conditions are less harsh, the population may even become locally maladapted (Fig. 4.2). This reflects the density-dependent nature of the selection. As the season goes on, the population density increases and the high-r individuals become less well-suited to the environment, resulting in local maladaptation. Therefore, a population crash is necessary to maintain a low population density and hence allow the high-r individuals to persist.

4.5 Effective population size

The differential equation model assumes an infinite population size, where evolution is deterministic. However, a real-world, finite population is subject to stochastic effects: both evolutionary (genetic drift) and demographic. If selection is sufficiently weak or the effective population size is sufficiently small, the evolution of a gene may be nearly neutral [28]. Selection is considered weak relative to neutral drift if the product of the selection coefficient and the effective population size $sN_e < 1$ [48].

The deterministic model above predicts that selection for a higher growth rate is stronger when environmental conditions are harsher and thus population densities are lower. Consequently, it's necessary to consider how the small effective population size may counterbalance the greater selection and lead to an increased influence of genetic drift on the evolution of the population. When population size fluctuates through time, as in this model, the effective

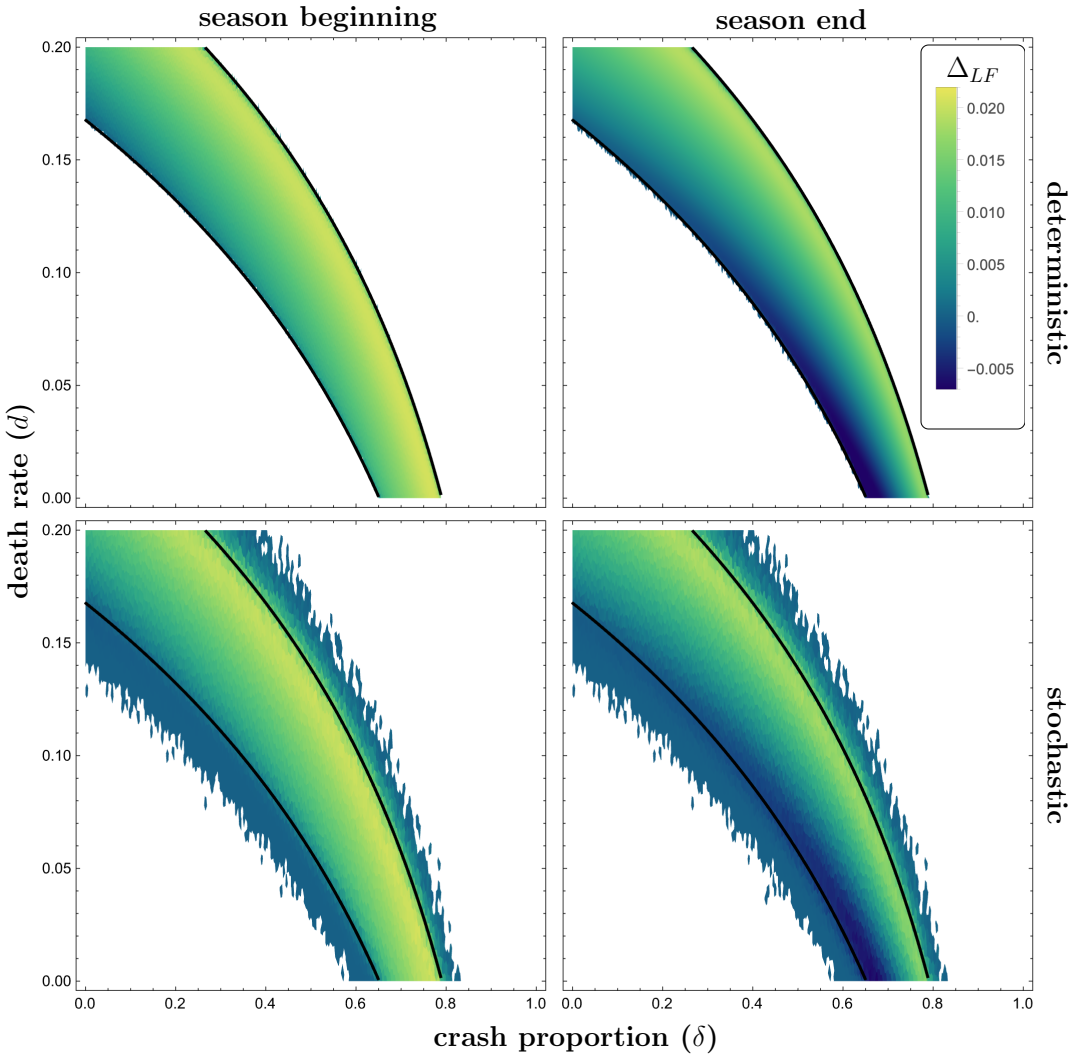

Figure 4.2: **Degree of local adaptation due to seasonal disruptions.** Measure of local adaptation is calculated according to Eq. 4.4. Black lines mark the point where the $\hat{p} = 0$ steady state changes from stable to unstable, calculated numerically from the deterministic model. For both the deterministic and stochastic models, local adaptation on the island is positive at the beginning of the season. Towards the end of the season, local adaptation becomes negative in less harsh environments, indicating maladaptation. Parameters: $b_A = 0.25$, $b_a = 0.2$, $X_A = 5000$, $X_a = 10000$, $M = 1$. Stochastic simulations were initialised with $N_A = 1000$ and $N_a = 1000$, and had a run time of 300.

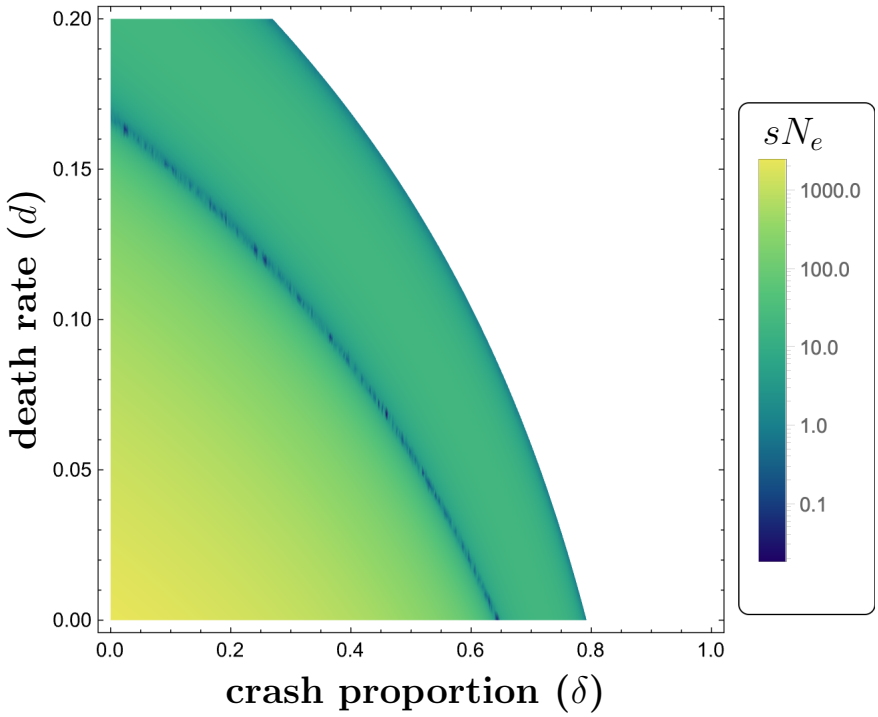

Figure 4.3: **Product of the selection coefficient and the effective population size.** For values near or less than 1, selection is considered weak relative to neutral drift. sN_e was not calculated in the parameter region where the island is a sink (white). Note values are shown on a log scale. Parameters: $b_A = 0.25$, $b_a = 0.2$, $X_A = 5000$, $X_a = 10000$, $M = 1$.

population size is given by the harmonic mean over the course of a single cycle [24]:

$$N_e = 2\pi \left[\int_0^{2\pi} \frac{1}{\hat{N}(t)} \right]^{-1}.$$

The selection coefficient is given by the difference in the fitnesses of the two alleles:

$$\begin{aligned} s &= W_A - W_a \\ &= b_A - b_a - \left(\frac{b_A}{X_A} - \frac{b_a}{X_a} \right) N_e. \end{aligned}$$

Figure 4.3 shows that selection is weakest along the areas of transition between coexistence and loss of the A allele. To understand how stochasticity might change the evolutionary outcomes in these parameter regions, we implement a finite population model of our island-mainland system.

4.6 Finite population model

We translate the dynamics presented in the deterministic case to a stochastic framework by implementing a Gillespie algorithm with the birth, death, and migration rates found in Table 4.1 [17]. This allows us to capture not only the stochasticity of genetic drift, but the effects of demographic stochasticity. At the end of a season, a proportion (δ) of the population is removed. Individuals are chosen to be removed at random, with no preference for one allele over the other. Simulations were performed across 7457 choices of the parameters δ and d with 50 replicates each.

Table 4.1: Birth, death, and migration rates.

Event	Rate
birth of individual i	$b_i N_i$
death of individual i	$\left(d + \frac{b_i}{X_i} N_T\right) N_i$
migration in of individual a	M

To quantify the local adaptation on the island, we measured the population size and allele frequency at the beginning and end of the last season of each simulation. We then used these values to calculate the local adaptation of the island at the beginning and end of the season, using the same 'local vs. foreign' definition (Eq. 4.4) as in the deterministic case. Figure 4.2 shows that pattern of local adaptation on the island predicted by the deterministic result is robust to genetic drift. A transient region arises near the boundaries of transition between coexistence and loss of the high-r, A allele, in which stochasticity allows for the occasional persistence of the A allele. This results in a small, non-zero average degree of local adaptation.

Chapter 5

Conclusion

In this thesis, I have used mathematical modelling and stochastic simulations to study the evolution of life-history traits under seasonal disruptions. Applying asymptotic analysis and Floquet analysis to a continuous-time model, I show that higher rates of reproduction can be favoured over higher competitive ability if the average amount of mortality over the course of a season reaches an intermediate level. If mortality is too low, higher competitive ability is favoured just as in a constant environment. If mortality is too high, the population will be driven to extinction. Notably, the timing of the mortality plays no role in the evolutionary outcome, with both impulsive population crashes and continuously varying death rates leading to the same outcomes. Conversely, varying the available resources in the population cannot result in selection for a high rate of reproduction. Restricting access to resources does not sufficiently reduce the population density to allow for the success of the high growth allele.

These theoretical findings align with observations in natural systems. They may explain why the drought-intolerant strain of *L. parviflorus*, with its greater competitive ability, is dominant in non-serpentine soil, despite temporal variability in rainfall [12]. Incorporating seasonal population crashes into a model of local adaptation to an island environment relative to a mainland, I show that the conditions for local adaptation to arise are similar to those necessary for r-selection in a single population. Simulations show that these results are robust to stochasticity.

The case study of the seaweed fly *C. frigida* is noteworthy in part because the chromosomal inversion allows a group of genes that confer an r- or K-selected phenotype to be passed

onto offspring together [44, 45]. Thus the inheritance pattern functionally behaves like that of a single biallelic locus, as in the model presented here. However such patterns of inheritance are rare; more often r- and K-selection emerges from a combination of phenotypes, all mediated by multiple genes. The simplifying assumption of a single locus model allows for better tractability and focuses on the question of what environmental conditions can or can not lead to broad patterns of r-selection over K-selection. Determining how more complex genetic architecture or trade-offs between more specific phenotypic traits may complicate the relationship of r/K selection and seasonality requires more complicated models and empirical work. Notably, a model which allows for a greater variety of phenotypes would show how intermediate life-history strategies, which are neither entirely r-selected nor entirely K-selected, might respond to different environmental disruptions.

The models presented here describe the evolution of only one of many possible life-history trade-offs shaped by density-dependent natural selection. Specifically, the models considered did not incorporate age structure as would be necessary for modelling to fully capture life-history evolution, as seasonality and mortality frequently both relate to the life cycle and age of individuals. A model incorporating age structure would explore questions about selective pressures on the rate of maturation and the importance of the timing of mortality relative to the life cycle. Additionally, these models assumed regular seasonality with a consistent severity. However, a consequence of climate change is irregular seasonality and more dramatic seasonal swings. As the work of Lande *et al.* has demonstrated, stochasticity also serves to shape life-history evolutionary dynamics [34, 35]. Incorporating a degree of stochasticity into the timing and severity of seasons may change the dynamics shown here. Alternatively, some environments experience seasons of great stability and seasons of large disruptions, motivating a model consisting of seasons of environmental stability and seasons of regular disruption. Both these cases may be of particular interest for stochastic simulations, where there are transient states in regions of higher or lower mortality (Fig. 4.2) where dynamics may easily shift in response to greater variability.

The work presented here extends classic life-history theory [40, 53], demonstrating how the seasonality can (in the case of seasonal mortality) and cannot (in the case of fluctuating resource abundance) favour the spread of r-selected life-history strategies. I show that r-

selected life-history traits are not favoured in all seasonal environments, but rather selection depends on the nature (how seasonality impact populations by changing population size, resource availability, or mortality rate), timing, and severity of seasonal disruptions. These results can be useful for understanding life-history evolution in experimental, agricultural, and natural systems. As anthropogenic climate change has increasingly dramatic impacts on seasonality and variability, understanding how temporal environmental variation shapes evolution in single populations as well as local adaptation across spatially-structured environments is increasingly important. The results and methods presented here establish a foundation on which this future work on the complex eco-evolutionary consequences of seasonality on the evolution of density-dependent traits can build.

Bibliography

[1] Gonzalo Albaladejo-Robles, Monika Böhm, and Tim Newbold. Species life-history strategies affect population responses to temperature and land-cover changes. *Glob. Change Biol.*, 29(1):97–109, 2023.

[2] Wyatt W. Anderson. Genetic Equilibrium and Population Growth Under Density-Regulated Selection. *Am. Nat.*, 105(946):489–498, 1971.

[3] Martín Andrade-Restrepo, Nicolas Champagnat, and Régis Ferrière. Local adaptation, dispersal evolution, and the spatial eco-evolutionary dynamics of invasion. *Ecol. Lett.*, 22(5):767–777, 2019.

[4] Ronald D. Bassar, Benjamin H. Letcher, Keith H. Nislow, and Andrew R. Whiteley. Changes in seasonal climate outpace compensatory density-dependence in eastern brook trout. *Glob. Change Biol.*, 22(2):577–593, 2016.

[5] François Blanquart, Oliver Kaltz, Scott L. Nuismer, and Sylvain Gandon. A practical guide to measuring local adaptation. *Ecol. Lett.*, 16:1195–1205, 2013.

[6] David H. Branson. Influence of a Large Late Summer Precipitation Event on Food Limitation and Grasshopper Population Dynamics in a Northern Great Plains Grassland. *Environ. Entomol.*, 37(3):686–695, 2008.

[7] Olivia J. Burton, Ben L. Phillips, and Justin M. J. Travis. Trade-offs and the evolution of life-histories during range expansion. *Ecol. Lett.*, 13(10):1210–1220, 2010.

[8] Brian Charlesworth. Selection in Density-Regulated Populations. *Ecology*, 52(3):469–474, 1971.

[9] Peter Chesson and Nancy Huntly. Temporal Hierarchies of Variation and the Maintenance of Diversity. *Plant Species Biol.*, 8(2-3):195–206, 1993.

[10] James F. Crow and Motoo Kimura. *An Introduction to Population Genetics Theory.* Harper & Row, New York, NY, 1970.

[11] Maxime Deforet, Carlos Carmona-Fontaine, Kirill S. Korolev, and Joao B. Xavier. Evolution at the Edge of Expanding Populations. *Am. Nat.*, 194(3):291–305, 2019.

[12] Emily L. Dittmar and Douglas W. Schemske. Temporal Variation in Selection Influences Microgeographic Local Adaptation. *Am. Nat.*, 202(4):471–485, 2023.

[13] David R. Easterling, Jenni L. Evans, Pavel Ya Groisman, Thomas R. Karl, Kenneth E. Kunkel, and Peter Ambenje. Observed Variability and Trends in Extreme Climate Events: A Brief Review. *Bull. Am. Meteorol. Soc.*, 81(3):417–426, 2000.

[14] Anthony S. Ferreira and Renato G. Faria. Predation risk is a function of seasonality rather than habitat complexity in a tropical semiarid forest. *Sci. Rep.*, 11(1):16670, 2021.

[15] Madhav Gadgil and Otto T. Solbrig. The Concept of r- and K-Selection: Evidence from Wild Flowers and Some Theoretical Considerations. *Am. Nat.*, 106(947):14–31, 1972.

[16] Kimberly J. Gilbert, Nathaniel P. Sharp, Amy L. Angert, Gina L. Conte, Jeremy A. Draghi, Frédéric Guillaume, Anna L. Hargreaves, Remi Matthey-Doret, and Michael C. Whitlock. Local Adaptation Interacts with Expansion Load during Range Expansion: Maladaptation Reduces Expansion Load. *Am. Nat.*, 189(4):368–380, 2017.

[17] Daniel T. Gillespie. Exact stochastic simulation of coupled chemical reactions. *J. Phys. Chem.*, 81(25):2340–2361, 1977.

[18] Richard Gomulkiewicz, Robert D. Holt, and Michael Barfield. The Effects of Density Dependence and Immigration on Local Adaptation and Niche Evolution in a Black-Hole Sink Environment. *Theor. Popul. Biol.*, 55(3):283–296, 1999.

[19] John B. S. Haldane. A mathematical theory of natural and artificial selection. (Part VI, Isolation.). *Math. Proc. Camb. Philos. Soc.*, 26(2):220–230, 1930.

[20] Megan C. Hall and John H. Willis. Divergent Selection on Flowering Time Contributes to Local Adaptation in Mimulus Guttatus Populations. *Evolution*, 60(12):2466–2477, 2006.

[21] Rebekah Hall, Akila Bandara, and Daniel A. Charlebois. Fitness effects of a demography-dispersal trade-off in expanding Saccharomyces cerevisiae mats. *Phys. Biol.*, 21(2):026001, January 2024.

[22] Oskar Hallatschek, Pascal Hersen, Sharad Ramanthan, and David R. Nelson. Genetic drift at expanding frontiers promotes gene segregation. *Proc. Natl. Acad. Sci. USA*, 104:19926–19930, 2007.

[23] Oskar Hallatschek and David R. Nelson. Gene surfing in expanding populations. *Theor. Popul. Biol.*, 73(1):158–170, 2008.

[24] Daniel L. Hartl and Andrew G. Clark. Darwinian Selection: Selection in a Finite Population. In *Principles of population genetics*. Sinauer Associates, 2007.

[25] Jeffrey A. Hutchings. Life-History Evolution in a Changing Environment. In Jeffrey A. Hutchings, editor, *A Primer of Life Histories: Ecology, Evolution, and Application*, pages 99–114. Oxford University Press, 2021.

[26] Olivia L. Johnson, Raymond Tobler, Joshua M. Schmidt, and Christian D. Huber. Fluctuating selection and the determinants of genetic variation. *Trends Genet.*, 39(6):491–504, 2023.

[27] Tadeusz Kawecki and Dieter Ebert. Conceptual issues in local adaptation. *Ecol. Lett.*, 7:1225–1241, 2004.

[28] Motoo Kimura. The neutral mutation-random drift hypothesis as an evolutionary paradigm. In *The Neutral Theory of Molecular Evolution*, pages 34–54. Cambridge University Press, 1983.

[29] Christopher A. Klausmeier. Floquet theory: a useful tool for understanding nonequilibrium dynamics. *Theor. Ecol.*, 1:153–161, 2008.

[30] Seraina Klopfstein, Mathias Currat, and Laurent Excoffier. The Fate of Mutations Surfing on the Wave of a Range Expansion. *Mol. Biol. Evol.*, 23(3):482–490, 2006.

[31] Colin T. Kremer and Christopher A. Klausmeier. Coexistence in a variable environment: Eco-evolutionary perspectives. *J. Theor. Biol.*, 339:14–25, 2013.

[32] Russell Lande. A Quantitative Genetic Theory of Life History Evolution. *Ecology*, 63(3):607–615, 1982.

[33] Russell Lande, Steinar Engen, and Bernt-Erik Saether. *Stochastic Population Dynamics in Ecology and Conservation*. Oxford Series in Ecology and Evolution. Oxford University Press, Oxford, 2003.

[34] Russell Lande, Steinar Engen, and Bernt-Erik Sæther. An evolutionary maximum principle for density-dependent population dynamics in a fluctuating environment. *Philos. Trans. R. Soc. Lond. B. Biol. Sci.*, 364(1523):1511–1518, 2009.

[35] Russell Lande, Steinar Engen, and Bernt-Erik Sæther. Evolution of stochastic demography with life history tradeoffs in density-dependent age-structured populations. *Proc. Natl. Acad. Sci. U.S.A.*, 114(44):11582–11590, 2017.

[36] William C. Leggett and James E. Carscadden. Latitudinal Variation in Reproductive Characteristics of American Shad (Alosa sapidissima): Evidence for Population Specific Life History Strategies in Fish. *J. Fish. Res. Board. Can.*, 35(11):1469–1478, 1978.

[37] Sébastien Lion and Sylvain Gandon. Evolution of class-structured populations in periodic environments. *Evolution*, 76(8):1674–1688, 2022.

[38] Bing Liu, Zhidong Teng, and Wanbo Liu. Dynamic behaviors of the periodic Lotka–Volterra competing system with impulsive perturbations. *Chaos Solit. Fractals.*, 31(2):356–370, 2007.

[39] Robert H. MacArthur. Some generalized theorems of natural selection. *Proc. Natl. Acad. Sci. U.S.A.*, 48(11):1893–1897, 1962.

[40] Robert H. MacArthur and Edward O. Wilson. *The Theory of Island Biogeography*. Princeton Univ. Press, 1967.

[41] Robert M. May. On Relationships Among Various Types of Population Models. *Am. Nat.*, 107(953):46–57, 1973.

[42] Mariah H. Meek, Erik A. Beever, Soraia Barbosa, Sarah W. Fitzpatrick, Nicholas K. Fletcher, Cinnamon S. Mittan-Moreau, Brendan N. Reid, Shane C. Campbell-Staton, Nancy F. Green, and Jessica J. Hellmann. Understanding Local Adaptation to Prepare Populations for Climate Change. *BioScience*, 73(1):36–47, 2023.

[43] Laurence D. Mueller, Pingzhong Guo, and Francisco J. Ayala. Density-Dependent Natural Selection and Trade-Offs in Life History Traits. *Science*, 253(5018):433–435, 1991.

[44] Claire Mérot, Emma L. Berdan, Charles Babin, Eric Normandeau, Maren Wellenreuther, and Louis Bernatchez. Intercontinental karyotype–environment parallelism supports a role for a chromosomal inversion in local adaptation in a seaweed fly. *Proc. Royal Soc. B.*, 285(1881):20180519, 2018.

[45] Claire Mérot, Violaine Llaurens, Eric Normandeau, Louis Bernatchez, and Maren Wellenreuther. Balancing selection via life-history trade-offs maintains an inversion polymorphism in a seaweed fly. *Nat. Commun.*, 11(1):670, 2020.

[46] Lucas A. Nell, Miriam Kishinevsky, Michael J. Bosch, Calvin Sinclair, Karuna Bhat, Nathan Ernst, Hamze Boulaleh, Kerry M. Oliver, and Anthony R. Ives. Dispersal stabilizes coupled ecological and evolutionary dynamics in a host-parasitoid system. *Science*, 383(6688):1240–1244, 2024.

[47] Brad M. Ochocki, Julia B. Saltz, and Tom E. X. Miller. Demography-Dispersal Trait Correlations Modify the Eco-Evolutionary Dynamics of Range Expansion. *Am. Nat.*, 195(2):231–246, 2020.

[48] Tomoko Ohta and Hidenori Tachida. Theoretical study of near neutrality. I. Heterozygosity and rate of mutant substitution. *Genetics*, 126(1):219–229, 1990.

[49] H. Allen Orr. Fitness and its role in evolutionary genetics. *Nat. Rev. Genet.*, 10(8):531–539, 2009.

[50] Jimmy H. Peniston, Gregory A. Backus, Marissa L. Baskett, Robert J. Fletcher, and Robert D. Holt. Ecological and evolutionary consequences of temporal variation in dispersal. *Ecography*, page e06699, 2023.

[51] Eric R. Pianka. On r- and K-Selection. *Am. Nat.*, 104(940):592–597, 1970.

[52] David Reznick, Michael J. Bryant, and Farrah Bashey. r- and K-Selection Revisited: The Role of Population Regulation in Life-History Evolution. *Ecology*, 83(6):1509–1520, 2002.

[53] Joan Roughgarden. Density-Dependent Natural Selection. *Ecology*, 52(3):453–468, 1971.

[54] Seth M. Rudman, Sharon I. Greenblum, Subhash Rajpurohit, Nicolas J. Betancourt, Jinjoo Hanna, Susanne Tilk, Tuya Yokoyama, Dmitri A. Petrov, and Paul Schmidt. Direct observation of adaptive tracking on ecological time scales in Drosophila. *Science*, 375(6586):eabj7484, 2022.

[55] Dolph Schluter. Ecology and the origin of species. *Trends Ecol. Evol.*, 16(7):372–380, 2001.

[56] Christoph Schär, Pier Luigi Vidale, Daniel Lüthi, Christoph Frei, Christian Häberli, Mark A. Liniger, and Christof Appenzeller. The role of increasing temperature variability in European summer heatwaves. *Nature*, 427(6972):332–336, 2004.

[57] Carla Sgrò and Ary Hoffmann. Genetic correlations, tradeoffs and environmental variation. *Heredity*, 93:241–248, 2004.

[58] Stephen C. Stearns. Life history evolution: successes, limitations, and prospects. *Sci. Nat.*, 87(11):476–486, 2000.

[59] Bernt-Erik Sæther, Thor Harald Ringsby, and Eivin Røskaft. Life History Variation, Population Processes and Priorities in Species Conservation: Towards a Reunion of Research Paradigms. *Oikos*, 77(2):217–226, 1996.

[60] Yvonne Teuschl, Constanze Reim, and Wolf U. Blanckenhorn. Correlated responses to artificial body size selection in growth, development, phenotypic plasticity and juvenile viability in yellow dung flies. *J. Evol. Biol.*, 20(1):87–103, 2007.

[61] Justin M. J. Travis, Tamara Münkemüller, Olivia J. Burton, Alex Best, Calvin Dytham, and Karin Johst. Deleterious Mutations Can Surf to High Densities on the Wave Front of an Expanding Population. *Mol. Biol. Evol.*, 24(10):2334–2343, 2007.

[62] Michael Turelli and Doug Petry. Density-dependent selection in a random environment: An evolutionary process that can maintain stable population dynamics. *Proc. Natl. Acad. Sci. U.S.A.*, 77(12):7501–7505, 1980.

[63] Mackenzie Urquhart-Cronish, Amy L. Angert, Sarah P. Otto, and Ailene MacPherson. Density-dependent selection during range expansion affects expansion load in life-history traits. *Am. Nat.*, 203(3):382–392, 2024.

[64] Alireza R. Vahidi, Zahra Azimzadeh, and Mohsen Didgar. An efficient method for solving Riccati equation using homotopy perturbation method. *Ind. J. Phys.*, 87(5):447–454, 2013.

[65] Farida Vasi, Michael Travisano, and Richard E. Lenski. Long-Term Experimental Evolution in Escherichia coli. II. Changes in Life-History Traits During Adaptation to a Seasonal Environment. *Am. Nat.*, 144(3):432–456, 1994.

[66] Easton R. White and Alan Hastings. Seasonality in ecology: Progress and prospects in theory. *Ecol. Complex.*, 44:100867, 2020.

[67] Meike T. Wortel, Elad Noor, Michael Ferris, Frank J. Bruggeman, and Wolfram Liebermeister. Metabolic enzyme cost explains variable trade-offs between microbial growth rate and yield. *PLoS. Comput. Biol.*, 14(2):e1006010, 2018.

[68] Sewall Wright. Evolution in Mendelian Populations. *Genetics*, 16:97–159, 1931.

[69] Yue Wu, Clare A. Saddler, Frank Valckenborgh, and Mark M. Tanaka. Dynamics of evolutionary rescue in changing environments and the emergence of antibiotic resistance. *J. Theor. Biol.*, 340:222–231, 2014.

[70] Sam Yeaman and Sarah P. Otto. Estabilishment and maintenanc of adaptive genetic divergence under migration, selection, and drift. *Evolution*, 65(7):2123–2129, 2011.

[71] Xiao Yi and Antony M. Dean. Bounded population sizes, fluctuating selection and the tempo and mode of coexistence. *Proc. Natl. Acad. Sci. U.S.A.*, 110(42):16945–16950, 2013.

Appendix A

Introductory Models

A.1 Patterns of density dependence in the logistic growth model

Here I present a discrete time logistic model of density-dependent selection on a haploid population to illustrate the patterns of density dependence of r and K. We consider a single gene with two possible alleles: A and a. Let N_A be the number of individuals with the A allele and N_a be the number of individuals with the a allele. The fitness of each allele is given by:

$$W_i(N) = (r_i + 1) - \frac{r_i}{K_i}N, \tag{A.1}$$

where N is the total population size, and r_i and K_i are the intrinsic growth rate and carrying capacity for the given allele. Additionally, we assume the there is a trade-off between the intrinsic growth rate and the carrying capacity:

$$r_A > r_a, \quad K_A < K_a.$$

Note that for small N, the second term in Eq. A.1 is small and therefore a large r confers the greatest fitness advantage. However as N increases, a large K becomes more advantageous in order to keep the second term small. The population size N_e when $W_A(N_e) = W_a(N_e)$ is labelled the effective population size [53]. Figure 2.1 in the main text shows that for population sizes below the effective population size, the high-r allele A has the fitness advantage, while for population sizes greater than the effective populations size, the high-K allele has a higher fitness. This density-dependent pattern in fitness translates to density-

dependence in selection. The selection coefficient for the A allele is given by:

$$\begin{aligned} S &= \frac{W_A(N) - W_a(N)}{\bar{W}(N)} \\ &= \frac{r_A\left(1 - \frac{N}{K_A}\right) + r_a\left(1 - \frac{N}{K_a}\right)}{1 + r_A\left(1 - \frac{N}{K_A}\right)p + r_a\left(1 - \frac{N}{K_a}\right)(1-p)}. \end{aligned}$$

We see that S is still dependent on N. If $r_A = r_a$, then the selection coefficient becomes:

$$S = \frac{2 - N\left(\frac{1}{K_A} - \frac{1}{K_a}\right)}{1 + r\left(1 - N\left(\frac{1}{K_A}p + \frac{1}{K_a}(1-p)\right)\right)}.$$

If $K_A = K_a$, then the selection coefficient is given by:

$$S = \frac{(r_A - r_a)\left(1 - \frac{N}{K}\right)}{1 + \bar{r}\left(1 - \frac{N}{K}\right)},$$

where r is the mean intrinsic growth rate. Therefore, selection coefficients for both r and K depend on N. That is, both the intrinsic growth rate and the carrying capacity experience density-dependent selection.

Using the fitness functions, we can define recursive equations for the frequency of the A allele, p, and the total population size, N:

$$p^{t+1} = p^t \frac{W_A(N^t)}{\bar{W}(N^t)}, \tag{A.2}$$

$$N^{t+1} = N^t\left[\bar{W}(N^t)\right]. \tag{A.3}$$

Setting $\Delta p = p^{t+1} - p^t = 0$ and $\Delta N = N^{t+1} - N^t = 0$, we find four equilibria:

$$\begin{aligned} \left(\hat{p}_1, \hat{N}_1\right) &= (0,0), \\ \left(\hat{p}_2, \hat{N}_2\right) &= (0, K_a), \\ \left(\hat{p}_3, \hat{N}_3\right) &= (1,0), \\ \left(\hat{p}_4, \hat{N}_4\right) &= (1, K_A). \end{aligned}$$

Using the Jacobian of p^{t+1} and N^{t+1} with respect to p^t and N^t, we find that the first and fourth equilibria are unstable and the second and third equilibria are stable. In other words, in a constant environment, the population will either go extinct or the high-K allele, a, will fix and the population size will approach the higher carrying capacity, K_a.

A.2 Density dependence of viability

A.2.1 Discrete-time model

The life cycle for a discrete time $b/V/K$ model of population growth is shown in Figure 2.3 of the main text, where N_i is the number of individuals with allele i, and primes do not indicate derivatives, but instead the population size after the next step in the cycle. From Eq. 2.1 in the main text, we can define the allele fitness as:

$$W_i(N) = V_i \left[1 + b_i \left(1 - \frac{N}{K_i}\right)\right],$$

and define the recursive equations for allele frequency and population size the same as Eq. A.2 and Eq. A.3 respectively.

To examine the selection on viability only, assume that birth rate and carrying capacity are the same for both alleles. Then the selection coefficient is given by:

$$\begin{aligned} S_V &= \frac{(V_A - V_a)\left[1 + b\left(1 - \frac{N}{K}\right)\right]}{(pV_A + (1-p)V_a)\left[1 + b\left(1 - \frac{N}{K}\right)\right]} \\ &= \frac{V_A - V_a}{\bar{V}}. \end{aligned}$$

This is completely independent of the population size. Contrast this with selection on birth rate and carrying capacity. Assuming viability and carrying capacity remain constant, the selection coefficient for birth rate is:

$$\begin{aligned} S_b &= \frac{V\left[1 + b_A\left(1 - \frac{N}{K}\right)\right] - V\left[1 + b_a\left(1 - \frac{N}{K}\right)\right]}{V\left[1 + b_A\left(1 - \frac{N}{K}\right)\right]p + V\left[1 + b_a\left(1 - \frac{N}{K}\right)\right](1-p)} \\ &= \frac{(b_A - b_a)\left(1 - \frac{N}{K}\right)}{\left(1 - \frac{N}{K}\right)\bar{b} + 1}. \end{aligned}$$

Holding viability and birth rate constant, the selection coefficient for the carrying capacity is:

$$S_K = \frac{V\left[1+b\left(1-\frac{N}{K_A}\right)\right] - V\left[1+b\left(1-\frac{N}{K_a}\right)\right]}{V\left[1+b\left(1-\frac{N}{K_A}\right)\right]p + V\left[1+b\left(1-\frac{N}{K_a}\right)\right](1-p)}$$

$$= \frac{b\left(\frac{N}{K_a}-\frac{N}{K_A}\right)}{\left(1-\frac{N}{K_A}p-\frac{N}{K_a}(1-p)\right)b+1}.$$

Both of these selection coefficients depend on the population size N. While the fitnesses for b, V, and K are all density dependent, only selection for b and K are also density-dependent.

A.2.2 Continuous-time model

Now consider the analogous continuous model. Here, rather than considering the viability V, we will use the death rate $d = 1 - V$. Since the carrying capacity (K) is defined as the equilibrium population size, which is changed by the inclusion of a death rate, we will instead use the variable X, which we call the growth rate. The differential equation for the change in the population with allele i is:

$$\frac{dN_i}{dt} = b_i N_i - \left(d_i + \frac{b_i}{X_i}N\right)N_i. \tag{A.4}$$

The Malthusian fitness of allele i is given as:

$$m_i = \frac{1}{N_i}\frac{dN_i}{dt} = b_i - \left(d_i + \frac{b_i}{X_i}N\right).$$

From this, the selection on the A allele in the continuous model is defined by:

$$S = m_A - m_a.$$

As with the discrete model, we first hold b and X constant to determine the selection coefficient for the death rate:

$$\begin{aligned} S_d &= b - \left(d_A + \frac{b}{X}N\right) - b + \left(d_a + \frac{b}{X}N\right) \\ &= -(d_A - d_a). \end{aligned}$$

This is not dependent on N, therefore selection on d, like selection on V, is not density-dependent. We can also see that selection on b and X will be density-dependent. Selection

on b in the continuous case is:

$$\begin{aligned} S_b &= b_A - \left(d + \frac{b_A}{X}N\right) - b_a + \left(d + \frac{b_a}{X}N\right) \\ &= \left(1 - \frac{N}{X}\right)(b_A - b_a), \end{aligned}$$

and selection on X in the continuous case is:

$$\begin{aligned} S_X &= b - \left(d + \frac{b}{X_A}N\right) - b + \left(d + \frac{b}{X_A}N\right) \\ &= b\left(\frac{N}{X_a} - \frac{N}{X_A}\right). \end{aligned}$$

We can also note that the selection coefficients in the continuous case are the same as the numerators of the selection coefficients in the discrete case. The difference here comes from the fact that the selection coefficient in the discrete case divides through by the mean fitness, whereas the continuous selection coefficient does not.

A.3 Polymorphisms in a periodic environment

Considering a discrete-time model of a diploid population under density-dependent selection, Roughgarden (1971) demonstrated that in a constant environment, the high-K allele will always fix when there is full dominance of either the high-K or the high-r allele. The full dominance cases are functionally the same as the haploid model described in appendix A.1. Only when the heterozygote had a higher carrying capacity than both homozygotes was it possible for a polymorphism to arise. When the heterozygote had a smaller carrying capacity than both homozygotes, no polymorphism could arise, but it was possible for the high-r allele to fix depending on the initial allele frequency. Additionally, Roughgarden demonstrated that introducing seasonality into the environment increased the range of cases in which a polymorphism may arise when the heterozygote's phenotype differs from both homozygotes. It also made possible a polymorphism in the case of full dominance, an outcome which cannot be achieved in a constant environment [53].

A haploid version of Roughgarden's periodic model is shown in Figure A.1. The life cycle consists of two seasons of growth, followed by a dormant season during which the population drops to some constant size N_0 [53]. The fitness functions are derived from a logistic growth model:

$$W_i(N) = (r_i + 1) - \frac{r_i}{K_i}N.$$

This system has three equilibria: $\hat{p} = 0$, $\hat{p} = 1$, and a polymorphic equilibrium. An equilibrium is stable if:

$$-1 < \left.\frac{dp_{t+1}}{dp_t}\right|_{p_t=\hat{p}} < 1.$$

Taking $N_0 \to 0$, we find that in extremely harsh environments the equilibrium $\hat{p} = 1$ is stable, so the high-r allele will fix. If we assume that $N_0 < K_A < K_a$, then to study the

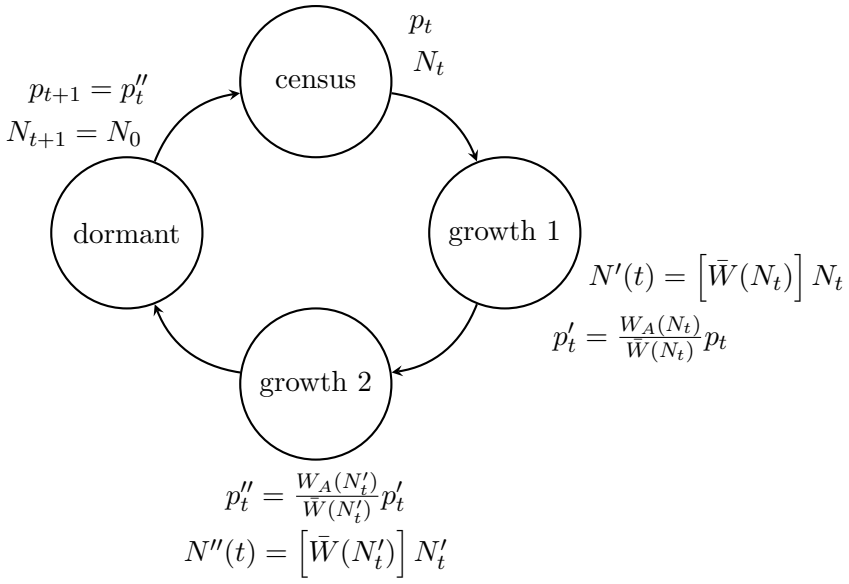

Figure A.1: **Single life-cycle for a haploid population with two growth seasons and a dormant season.** N represents the total population size, p represents the frequency of the high-r allele, W_i are the fitness functions of each genotype, and N_0 is the fixed population size the population drops to a every dormant season. Primes do not represent derivatives, but indicate the next step in the life-cycle.

system's behaviour in nice environments we take the limit $N_0 \to K_A$. In this case, the $p^* = 0$ equilibrium is stable, so the high-K allele fixes. Therefore a polymorphic equilibrium may only arise in a moderate environment. Figure A.2 shows the stability of the steady state $\hat{p}$ as N_0 changes for three different values of K_a, the carrying capacity of the big-K allele. As the larger carrying capacity increases, the environmental harshness necessary to yield a polymorphism increases. Similarly, Figure A.3 shows the stability with different values of r_A: as the growth rate of the big-r allele increases, the necessary environmental harshness decreases. In all cases, the window for a stable polymorphism is small. The majority of environmental conditions lead to fixation or loss.

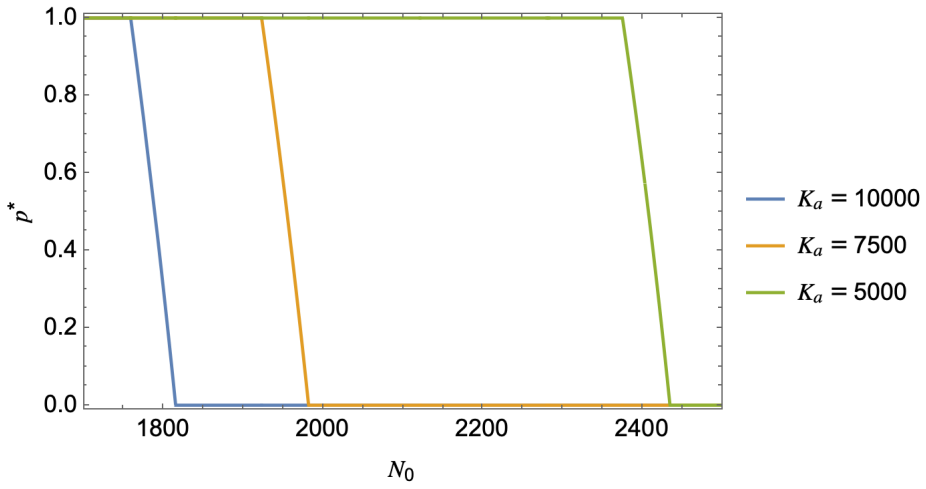

Figure A.2: **Stable steady state allele frequencies over a range of environmental harshnesses for three different big-K allele carrying capacities.** Parameter values are as follows: $K_A = 3500$, $r_A = 0.8$, $r_a = 0.4$

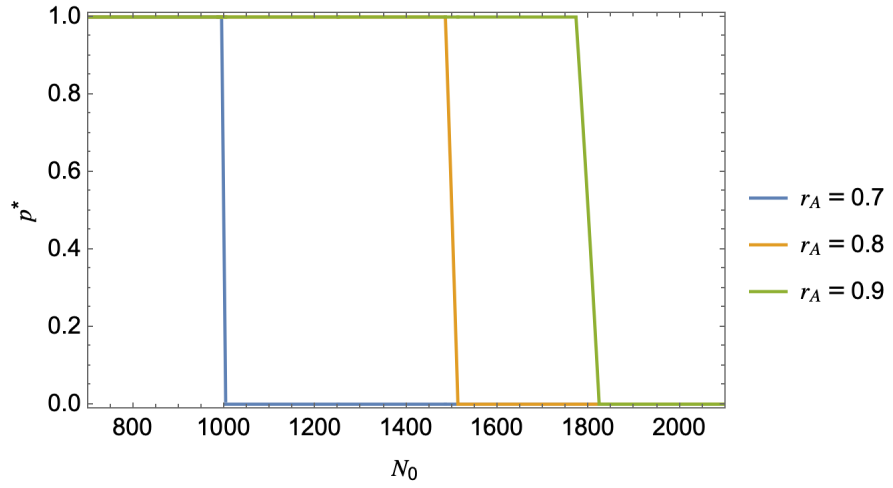

Figure A.3: **Stable steady state allele frequencies over a range of environmental harshnesses for three different big-r allele growth rates.** Parameter values are as follows: $K_A = 3500$, $K_a = 5000$ $r_a = 0.6$

Appendix B

Mathematica analysis of island-mainland model

Description:

Mathematica notebook containing the analysis for the island-mainland model of local adaptation of life-history traits. A PDF version of the notebook is also included.

Filename:

Hall_Rebekah_mathematica_notebook.zip

Summit link:

https://summit.sfu.ca/item/38288